UNCLASSIFIED

AD 296 016

Reproduced by the

ARMED SERVICES TECHNICAL INFORMATION AGENCY
ARLINGTON HALL STATION
ARLINGTON 12, VIRGINIA

UNCLASSIFIED

Best
Available
Copy

Ford Motor Company,
AERONUTRONIC DIVISION

Publication No. U-1929

RESEARCH LABORATORY

ANNUAL TECHNICAL REPORT

INFRARED RADIATION EMITTED BY HOT GASES AND ITS TRANSMISSION THROUGH SYNTHETIC ATMOSPHERES

Prepared for: Advanced Research Projects Agency
The Pentagon
Washington 25, D. C.

Under Contract: NOnr 3560(00)

Prepared by: Darrell E. Burch
David A. Gryvnak

31 October 1962

ABSTRACT

Measurements of the infrared emission of CO_2 and H_2O near 3700 cm^{-1} and near 2350 cm^{-1} have been made at 900°K, 1200°K and 1500°K with pressures varied between approximately 5 and 1500 mm Hg. Samples were contained in a sample cell 7.75 cm long and heated by molybdenum wire furnace. Investigations were made of absorption of radiation from hot CO_2 by cold CO_2 and compared with the absorption of radiation from a continuous source. Results of the measurements are presented in considerable detail in tables and figures.

TABLE OF CONTENTS

LIST OF TABLES

LIST OF FIGURES

LIST OF FIGURES (CONT.)

SECTION 1

INTRODUCTION

General Discussion

More fundamental information about the emission of infrared radiation from flames and its transmission through the atmosphere is clearly needed. The objective of the present experimental investigation is to provide basic information about the emission of CO_2 and H_2O, the two most important constituents of flames, and about the transmission of the emitted radiation through atmospheric paths containing these same two species. A typical flame shows a region of strong emission by CO_2 near 2350 cm^{-1} (4.3 microns) and another by CO_2 and H_2O near 3700 cm^{-1} (2.7 microns). This report is devoted to measurements made in these two spectral regions.

A furnace has been designed and built to heat samples composed of H_2O and CO_2 and other gases to temperatures as high as 2000°K. The sample gas is contained in a small platinum cell with sapphire windows, and the temperature of the sample is uniform to approximately ± 10°K. Virtually any mixture of H_2O, CO_2, and any gas which does not react with copper tubing can be investigated at any pressure between approximately 3 and 1500 mm Hg. The measurements have been made with the a of determining the dependence of emission on the temperature, the optical thickness of the emitting gas, the partial pressure of the emitting gases, and the partial pressure of other non-emitting gases which are present. Nitrogen has been used as a non-emitting foreign gas. It is believed that the information presented in this report, along with that which will result from continued investigations, will be invaluable in making calculations of the emission from flames which are larger than can be produced in the laboratory, and are non-uniform in temperature and in composition. The type of information provided by the present investigation is essential for the development of proper band models necessary for such calculations.

Since the objective is to obtain quantitative data on effects of pressure, temperature, etc., it was decided to investigate samples heated by a furnace rather than flames. Much better control of samples contained in a cell heated by a furnace is possible. The temperature and composition can be kept uniform throughout the sample, while these parameters are variable throughout a flame. The temperature, pressure, and composition can also be varied over much wider ranges. Results of the CO_2 and H_2O measurements are presented in Sections 3 and 4, respectively.[2]

A second phase of the study involves the transmission of radiation through synthetic atmospheres. Considerable work has been done on the transmission of radiation from continuous sources, such as glowers and hot filaments, through atmospheric paths. However, the problem is further complicated when the source of radiation is a gas flame containing the same species as the absorbing gas. The complication results from the fact that many of the emission maxima occur at the same frequencies as the absorption maxima. A detailed discussion of this effect is presented in Section 5 along with the results of several measurements which have been made.

Since the investigations are being continued, very little analysis of the data is presented in this report. The data are presented in considerable detail in the form of tables and figures so that they can be used conveniently by other workers for comparison, or for a basis for theoretical calculations. Further reports on this investigation will contain a considerable amount of analysis; and comparisons will be made with results of related investigations by workers at General Dynamics[1], Warner and Swasey[2], University of California[3], Israel Institute of Technology[4], and Armour Research Institute[5]. Effects of temperature, pressure, optical thickness, etc. will be determined and the usefulness of different band models will be considered.

Units, Symbols, and Definitions

The Greek letter ν is used to denote the frequency of radiation in wavenumber (cm^{-1}), the number of waves per centimeter in vacuum. Wavelengths are measured in microns and denoted by λ. Frequencies in cm^{-1} can be found by dividing 10^4 by the wavelength in microns.

$k(\nu)$ is the true absorption coefficient at frequency ν as it would be observed with an instrument having infinite resolving power. Wherever "true" is used with absorption coefficient, transmittance or

emissivity, it corresponds to infinite resolving power. True transmittance is given by $\exp(-k(\nu)u)$, where u is the optical thickness.

$T(\nu)$ is the transmittance of a sample measured at frequency ν with a continuous source and a spectrometer having finite slit width. The transmittance of a gas sample is the ratio of the radiation transmitted by the gas to that incident on it. Absorptance is denoted by $A(\nu)$ and is $1-T(\nu)$. Emissivity $\epsilon(\nu)$ is also $1-T(\nu)$; absorptance is used with reference to cold gases for which the interest is in the absorption of radiation. Emissivity is used with reference to hot gases whose radiation characteristics are being studied. The emissivity of a gas is the ratio of the emitted radiant power to the radiant power from a blackbody at the same temperature. $\bar{\epsilon}$ is used to denote the average value of $\epsilon(\nu)$ over a specified interval.

$N(\nu)$ denotes spectral radiance in watts $ster^{-1}$ cm^{-2} cm^{1}. N denotes radiance in watts $ster^{-1}$ cm^{-2}; either for all frequencies or over a specified interval. Different subscripts and superscripts used with the symbols described above refer to specific cases. For example $N^B(\nu)$ denotes the spectral radiance of a blackbody. $T_C(\nu)$, $T_H(\nu)$ and $T_{HC}(\nu)$ denote transmittances of a cold gas, a hot gas, and a hot and cold gas in series, respectively. When an asterisk is used with a symbol for transmittance such as $T_C^*(\nu)$, it denotes the transmittance that would be observed with a hot gas source.

Total pressures are denoted by P, and partial pressures of individual gases by $p(CO_2)$, $p(H_2O)$, etc. All pressures are measured in mm Hg.

Values of optical thickness u for CO_2 samples are determined in atmos cm STP by

$$u \text{ (atmos cm STP)} = \frac{p(CO_2)}{760} \; L \; \frac{\theta_o}{\theta} . \qquad (1\text{-}1)$$

where L is the length of the sample in cm, θ_o is standard temperature, 273^oK; and θ is the gas temperature in ^oK. Dividing by 760 converts the pressure to atmospheres. The temperature factor θ_o/θ is to be noted since many authors do not apply it in their calculations. In the present investigation this factor is used so that a given value of u in atmos cm STP corresponds to the same value in moles per cm^2 or gms per cm^2, regardless of the temperature. In the case of CO_2, values of optical thickness can be converted from atmos cm STP to gms per cm^2 by multiplying by 1.96×10^{-3}.

In the case of H_2O, values of u are expressed in precipitable cm (pr. cm), which is numerically equivalent to gms per cm^2, and can be calculated by

$$u \text{ (pr. cm } H_2O) = \frac{p(H_2O)}{760} \; \frac{L\,\theta_e}{\theta} \; 5.90 \times 10^{-4} \qquad (1\text{-}2)$$

The term optical thickness is used instead of absorber concentration which has been used for the same quantity by some workers, including the authors[7]. Optical thickness has been chosen since it seems to be more descriptive; units used in the present report are based on those used most often by other investigators doing similar work.

SECTION 2

EXPERIMENTAL

Apparatus

A diagram of the optical components of the apparatus is shown in Figure 2-1. Radiation from a Nernst glower passes a 13 cps chopper and is focused near a small absorption cell inside the furnace. The absorption cell is not shown in Figure 2-1, but the sapphire windows which fit it are shown. After passing through the cell, the radiation travels on through the furnace and an image of the glower is formed on the slit of a Perkin-Elmer Model 99 monochromator. The absorptance at any frequency is obtained by comparing the signal observed with a sample in the hot cell to that observed with the cell evacuated. Since the furance is between the chopper and the monochromator, radiation from it is not modulated and is not detected. Absorption by the windows is accounted for by the comparison of the spectra. If one were to use the hot gas directly as a radiation source, error would arise from radiation emitted by the windows or reflected from them. This radiation could not be very accurately accounted for by comparing the signal with a sample in the cell to that obtained with the cell evacuated. Each window would not only emit and scatter radiation into the instrument; it would also absorb a portion of the radiation from the preceding components. For example, the cell window on the side next to the monochromator would absorb part of the radiation emitted by the gas and by the window on the opposite side of the gas. Similarly, the sample gas would absorb part of the radiation from one window and none from the other. Thus, it is apparent that the contribution of the radiation due to the windows would change with the gas sample and would be very difficult to determine.

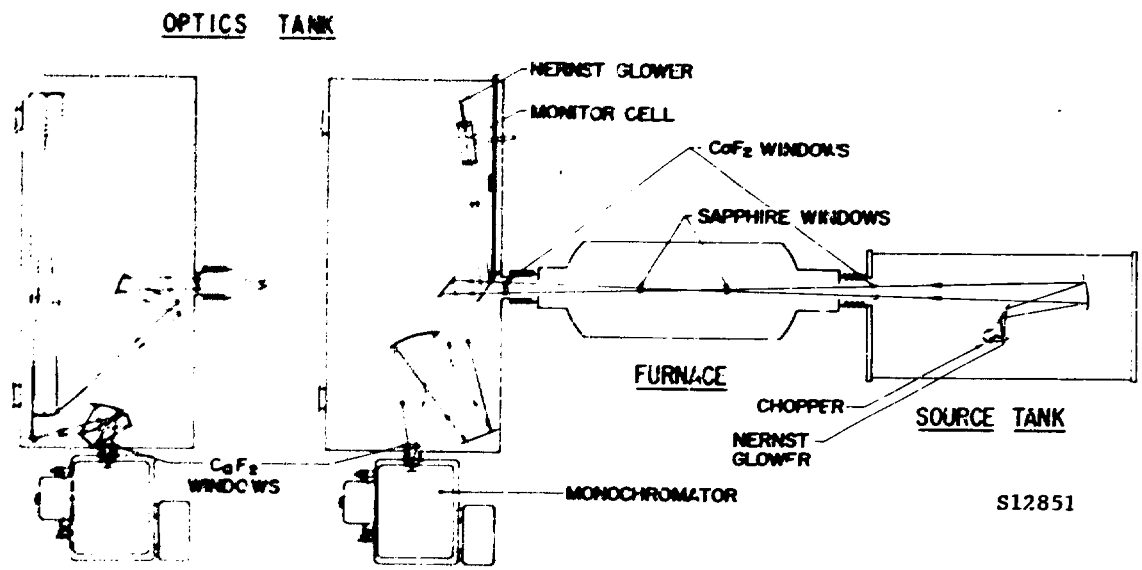

FIGURE 2-1. OPTICAL DIAGRAM OF APPARATUS. RADIATION FROM A NERNST GLOWER IS FOCUSED NEAR THE CENTER OF A SAMPLE CELL WHICH IS LOCATED IN THE FURNACE. THE RADIATION PASSES ON THROUGH THE FURNACE AND AN IMAGE OF THE GLOWER IS FORMED ON THE SLIT OF A PERKIN-ELMER PRISM MONOCHROMATOR. THE SAPPHIRE WINDOWS SHOWN ARE THE WINDOWS OF THE SAMPLE CELL, AND THE SAMPLE IS CONFINED TO THE REGION BETWEEN THEM. ARGON FILLS THE TWO END SECTIONS OF THE FURNACE BETWEEN THE SAPPHIRE AND CaF_2 WINDOWS. A FLAT MIRROR CAN BE MOVED INTO THE PATH OF THE BEAM LEAVING THE FURNACE SO THAT IT DIRECTS LIGHT FROM A NERNST GLOWER ONTO THE SLITS OF THE MONOCHROMATOR. THE LEFT-HAND PORTION OF THE FIGURE SHOWS THE OPTICAL ARRANGEMENT USED TO OBTAIN LONG PATH LENGTHS WHEN THE OPTICS TANK WAS USED AS AN ABSORPTION CELL.

ONTO THE SLITS OF THE MONOCHROMATOR. THE LEFT-HAND PORTION OF THE FIGURE SHOWS THE OPTICAL ARRANGEMENT USED TO OBTAIN LONG PATH LENGTHS WHEN THE OPTICS TANK WAS USED AS AN ABSORPTION CELL.

Since, according to Kirchhoff's Law, the emissivity of a body in thermal equilibrium is equal to its absorptance, the emissivity can be determined from the measurements. The spectral radiance can then be calculated from the product of the emissivity and the spectral radiance of a blackbody at the temperature of the sample.

In order to reduce errors in emissivity measurements arising from absorption by atmospheric gases, all the optical path except for that in the monochromator and the furnace is confined to a source tank and an optics tank. Either tank can be evacuated and filled with gas to any desired pressure less than atmospheric; the optics tank is usually evacuated, while the source tank is evacuated and then filled with dry nitrogen. While making some measurements of the type described in Section 5, absorbing gas is put in the optics tank. The source tank is not operated under vacuum in order to avoid possible trouble with the chopper and because of a tendency of the Nernst glower to evaporate and form a film on the mirrors. The lid of the monochromator is connected to the window at the end of the optics tank by means of a bellows to reduce leakage of air into the region under the lid, which is flushed with dry nitrogen at the rate of about 3 liters per minute. Under these conditions, it is possible to reduce the maximum absorptance in the regions of the CO_2 bands at 2350 cm^{-1} and the H_2O bands at 3700 cm^{-1} to about 0.01 or 0.02.

The monochromator was originally placed inside the optics tank where it could be evacuated and filled with dry nitrogen, but later it was decided to use it outside the tank, as shown in Figure 2-1, to avoid complications in making slit adjustments and in scanning the Littrow drive.

The optical system for the optics shown in the left-hand portion of Figure 2-1 is used when it is desired to have a rather long path of absorbing gas in "series" with the gas in the furnace. An image of the glower is formed adjacent to the single mirror of a multiple-pass mirror system similar to that described by White[6]. In the studies using this system, which are described in Section 5, the number of passes could be varied from outside the tank without opening it or without changing the gas in it. The maximum number of passes used was 24, which corresponds to a total path of more than 2600 cm within the optics tank.

The image of the glower formed near the hot cell is enlarged by a factor of approximately three. This image is then reduced by about the same factor, giving an image approximately 0.4 cm high on the slit of the monochromator. By decreasing the f-ratio in this manner,

the beam entering the monochromator "fills" more than 80 percent of the prism. Since there is some vignetting, and since the height of the slits is about 1 cm compared to the image height of 0.4 cm, the monochromator is only about 30 percent filled. In an optical system such as this, the maximum resolving power is limited by the minimum slit width compatible with the desired signal-to-noise ratio. The resolving power is approximately proportional to the reciprocal of the physical slit width, and the signal is nearly proportional to the square of slit width. Thus, the maximum resolving power is about one-half as great as if the monochromator were completely filled. Since high resolving power is not essential in the present study, the factor of two which is lost is not considered important.

It would be possible to more nearly fill the monochromator optics by using an image-splitter or by increasing the aperture of the furnace; but the advantages that would be realized do not appear to justify the inconvenience. If the aperture of the furnace were increased by enlarging the opening, more power would be required and it would be much more difficult to maintain uniform temperature over as long a portion of the furnace. An image-splitter which would split an image of the glower vertically into two halves and re-image them, one above the other, could make use of more of the height of the slit. Such a device takes advantage of the fact that the image formed on the slits is usually much wider than the slit opening; some of the radiation that would ordinarily be wasted is then used to form a higher image without increasing the f-ratio of the beam. However, in view of the fact that the optical system is already complex, the further complication of an image-splitter did not seem justified.

In the normal operation of a Perkin-Elmer double-pass-monochromator, the beam is chopped internally after one pass at a point conjugate to the exit slit. For any setting of the Littrow mirror, there is some frequency which passes through the exit slit after only a single pass (actually two passes through the prism, since the beam traverses the prism twice in a single pass instrument and four times in a double pass), but the single pass radiation is not detected because it has not been chopped. However, if the beam is chopped externally, as in the present study, some modifications must be made in order to avoid simultaneous detection of radiation at two different frequencies, one single passed and one double passed. To double pass the instrument while using the external chopper, the bottom halves of the entrance and exit slits were blocked off. The single-pass radiation from the top half of the entrance slit is focused on the bottom of the exit slit which is blocked off. Single-pass radiation is therefore not detected. During the second pass, the image of the entrance slit is reinverted so that the double-pass radiation

entering the upper half of the entrance slit passes through the upper half of the exit slit. Since the height of the image of the Nernst glower formed at the entrance slits is less than half the height of the slits, no loss in signal was introduced by blocking half of each slit.

The instrument was double passed to take advantage of the increased dispersion. Also the frequency calibration and the dispersion are the same as when the instrument was double passed while using the internal chopper in conjunction with other optical systems, such as the Nernst glower and monitor cell in the optics tank. When using the external chopper the internal chopper is positioned so that it is out of the beam. A window has been added to the lid of the monochromator so that the internal chopper can be viewed while positioning it.

With the monochromator double passed in this manner, the "scattered light" was less than 0.1 percent of the total radiation near the 3700 cm^{-1} region and was about 0.5 percent in the region of the strong CO_2 absorption near 2350 cm^{-1}. The amount of scattered light was determined by comparing the recorder deflection with the entrance slits covered to that with a sample of CO_2 large enough to produce complete absorption. Since the amount of scattered light was so small, it could be accounted for sufficiently well to avoid significant error.

If the physical slit width of the monochromator were kept constant while scanning over the entire region of CO_2 absorption near 2350 cm^{-1}, the recorder deflection on the low frequency side was found to be only about 20 percent as great as that on the high frequency side. In order to reduce the change in deflection from one side of the absorption region to the other, the slit servo-mechanism built for the monochromator by Perkin-Elmer was used to open the slits automatically according to a pre-determined program. A nonlinear electrical cam which was custom made in our laboratory was found to produce a reasonably smooth background when used with the Perkin-Elmer slit servo. The physical slit width was kept constant while scanning the region near 3700 cm^{-1} since the change in recorder deflection from one side of the region of absorption to the other side was less than for the region near 2350 cm^{-1}. A further reason for using constant slits at higher frequencies is that the slits are narrower and a small error in the servo mechanism would produce a larger error in the recorded signal.

Table 2-1 gives values of spectral slit width $\Delta\nu$ at several frequencies for the different slit programs used. The values are based on curves in the instrument instruction manual relating $\Delta\nu$ to the physical slit width, and are one-half the width of the total spectral interval passed by the slits. These values are approximately the same as would be obtained by using the Rayleigh criterion. In the discussion of the results, reference is made to the resolution schedule which was used while obtaining the data.

TABLE 2-1

RESOLUTION SCHEDULES

Wavenumber cm^{-1}	($\Delta\nu$) in cm^{-1}			
	A	B	C	D
1800	3.7	5.0		
2000	3.5	4.8		
2200	3.2	4.6		
2400	3.1	4.4		
2600		4.6		
2800			2.9	4.2
3000			3.5	5.2
3200			4.3	6.4
3400			5.1	7.6
3600			6.0	8.9
3800			7.0	10.4
4000			8.1	12.0
4200			9.2	13.7
4400			10.4	15.5

The synchronous motors, which drive the recorder chart and the monochromator Littrow drive, were replaced by selsyns. Both of these selsyns are now driven from the same transmitter which is powered by a variable speed d.c. motor. With this arrangement the recorder chart and Littrow drive are synchronized so that the frequency calibration on a spectrum remains the same and the scanning speed can be varied. The scanning speed is manually controlled so that there is sufficient time for the recorder to respond and give a true reading. Portions of the spectrum with little or no structure can be scanned as much as 5 times faster than the portions containing considerable structure. By varying the speed the scanning time is reduced to about 60 or 70% of the time required for a constant scanning speed which is determined by the region having the most structure.

A gas handling system, which is described in considerable detail in Appendix B, was designed to deliver gas samples to the sample cell in the furnace at any desired pressure between approximately 3 and 1500 mm Hg. Virtually any gas mixture, including water vapor, which will not react with copper tubing can be produced and flowed continuously through the sample cell at a regulated pressure. All the components which contain sample gas can be heated to approximately 140°C in order that H_2O can be investigated without condensation in the lines. Argon which is inactive in the infrared is continuously flushed through the section of the furnace around the sample cell. The argon pressure is maintained very close to that of the sample in order to avoid rupturing the thin sapphire windows of the sample cell and to reduce leakage past them. The windows are only 0.3 mm thick so that absorption of radiation by them is kept to a minimum. Absorption by sapphire becomes important at high temperature at frequencies below about 2200 cm^{-1} ($\lambda > 4.5\mu$).

Both the sample gas and the argon are flushed continuously to avoid accumulation of either of these gases in the wrong section of the furnace, and to carry away any impurities that might arise from slow reactions or from de-gassing from the walls of the furnace, which might occur because of the high temperatures. A small absorption cell and a separate radiation glower were employed in order to monitor the composition of the gases by observing their absorption spectra. The arrangement is shown in Figure 2-1. A small flat mirror located inside the optics tank can be moved into the path of the beam coming from the furnace, thus blocking it from the monochromator. When in this position, the mirror directs light from a Nernst glower onto the monochromator. Located in the beam is a small absorption cell, labeled as a monitor cell, which is connected to the gas handling system. The primary purpose of the monitor cell is to contain samples of gas which can be bled

from either the hot cell in the furnace or from the argon sections. Spectra of these samples can be obtained periodically to monitor the composition of these gases. For example, the purity of the argon is monitored to check for possible leakage of excessive amounts of sample gas into the argon section. By comparing the spectra with others obtained for known mixtures in the cell, it is possible to estimate the amount of sample gas present. On the basis of checks made while obtaining the data presented in this report, it was found that there was usually less than 0.05 of one percent sample gas in the argon. Error arising from the presence of this gas is therefore small. Similar checks of gases bled from the hot cell indicated that the deviation from purity was usually less than could be detected. The purity was therefore believed to be greater than 98%. While obtaining spectra of samples in the monitor cell, the internal chopper was used.

Because of condensation in the cold lines, water vapor from the hot cell could not be bled into the monitor cell. However, the same handling procedures and flow rates were used for water vapor as for CO_2 and it was assumed that negligible error was introduced by leakage.

Recording of Data

Before and after the spectra of a series of samples were obtained, background spectra were run with the sample cell evacuated but with all other experimental conditions the same as those for the samples. The frequency interval covered by the background spectra was somewhat wider than that over which the largest sample would absorb. In the case of CO_2 samples the region near 2350 cm^{-1} and the one near 3700 cm^{-1} were scanned separately. When studying H_2O, the region near 3700 cm^{-1} was scanned in one continuous spectrum.

Samples were usually divided into sets composed of a given mixing ratio at different pressures. In general, the first sample was at the lowest pressure at which the absorption was sufficiently great to be measured with reasonable accuracy. Succeeding samples were at higher pressures, where the pressures were increased by a factor of approximately two between samples. After the sample pressure was changed, but before a spectrum was scanned, the flow rates of the sample gas and argon were adjusted to some predetermined optimum value and the flow was maintained for a few minutes. Immediately after each spectrum was scanned the recorder deflection was checked at a few key frequencies within the band. If the deflections at these frequencies were the same as were observed during the scan, it was assumed that

there was a negligible drift. In cases of excessive drift the spectrum was re-run.

Reduction and Presentation of Data

Curves which represent recorder deflection for no sample absorption were superimposed on each sample spectrum by tracing the appropriate background spectrum. There were always at least two background spectra for each sample, one obtained before the sample spectrum and one after it. Comparison of the different backgrounds provided a check for drifts within any one spectrum and for other possible "long term" variations which might occur between the times they were obtained.

There is, of course, some uncertainty in fitting a background to a sample spectrum. This uncertainty is particularly noticeable in the wings of a band if the absorptance decreases very slowly. The error which might arise in any individual spectrum can be reduced by "nesting" all the curves belonging to a set of samples. For example, if samples of a given mixing ratio at 9 different pressures were studied, the spectra of several of these samples can be superimposed. Since it is known that the absorption at any frequency increases with increasing pressure, the absorption indicated by any single sample should be consistent with that of the other samples. Better accuracy can be attained by this technique, since information from several spectra is used to determine the spectrum of any single sample.

After the backgrounds have been drawn the information is put in digital form for use on an IBM 7090. Values of recorder deflection are recorded on punched cards for enough points to define the curve; the points at which any curve is read are chosen according to the amount of structure and occur at variable density along the curve. As an approximate criterion, points are read at every maximum and minimum and at points in between so that straight lines joining them will not deviate from the curve by an amount corresponding to more than 1/4 percent transmittance. The same criterion is used for the background curve as for the sample curve, and no attempt is made to read both curves at the same frequencies. Each card contains information about the recorder deflection and about the x-value, from which the frequency is calculated. A program for the IBM 7090 has been developed to provide the following output for each sample whose emission is being studied.

(1) Values of emissivity $\epsilon(\nu) = 1 - T(\nu)$, and frequency in cm^{-1} at all points where the sample spectrum was read.

(2) Values of $N(\nu)$ at the same frequencies; $N(\nu)$ is the spectral radiance of the gas computed from the product of $\epsilon(\nu)$ and the spectral radiance of a blackbody at the temperature of the gas.

(3) Values of $\bar{\epsilon}$, the average emissivity over 5 cm^{-1} intervals. These are determined by averaging values of $\epsilon(\nu)$ which are calculated at integral wave numbers as an intermediate step.

(4) Values of N the radiance in watts cm^{-2} $ster^{-1}$ for the 5 cm^{-1} intervals. These values are determined from the product of $\bar{\epsilon}$ for the same interval and $5N^B(\nu_o)$, where $N^B(\nu_o)$ is the spectral radiance at the center of the interval of a blackbody at the same temperature as the gas. Since the spectral radiance of a blackbody is nearly constant over a 5 cm^{-1} interval for the temperatures and frequencies covered in the present study, the simple product is a very good approximation to the radiance of the interval.

(5) Values of $\bar{\epsilon}$ for 50 cm^{-1} intervals, determined by one-tenth the sum of the values of $\bar{\epsilon}$ for the ten 5 cm^{-1} intervals.

(6) Values of N for 50 cm^{-1} intervals, determined from the sum of the values for the ten 5 cm^{-1} intervals.

In information contained in (1) and (2) are included in the computer output in tabular form and on cards which can be used with an automatic plotter, while the information in (3), (4), (5), and (6) is presented in tabular form only. The curves of emissivity shown in Sections 3 and 4 were plotted from the punched cards, but the remainder of the output described in (1) and (2) above is not included in this report. The emissivity curves are presented rather than photographs of the original spectra which have a nonlinear wave number scale and for which the background curve corresponding to 100% transmittance is not constant. Tabular information from (3), (4), (5) and (6) above is presented in Sections 3 and 4.

The results of the investigation of the transmission of radiation from hot CO_2 through cold CO_2 are presented in a different manner in Section 5 along with a discussion of experimental techniques, data, and the theory involved.

The major portion of the results obtained are presented in this report in a manner that should be convenient for workers who need the raw data to compare with their results, or for others who are interested in fitting data to various band models. Very little analysis is presented here since more data will be obtained in the near future and a detailed analysis of all the data will be performed at that time.

Errors and Accuracy

In a study such as this there are certain sources of error which arise from sampling, from data recording, and from data analysis. Uncertainties in sampling are somewhat larger in the present study than in studies that are not complicated by the high temperatures and by the necessity of flowing the sample continuously while making measurements. The recorded temperature of the sample of hot gas is accurate to approximately $\pm$ 10°K; this uncertainty causes approximately $\pm$ 1% error in the calculation of optical thickness, which is inversely proportional to temperature at a given pressure.

Approximately $\pm$ 1% error in the calculation of optical thickness arises from the uncertainty in the length of the sample cell at high temperatures. Available data on the coefficient of thermal expansion of the cell material only covers temperatures to 1000°C. The cell length at the higher temperatures was calculated by assuming the same coefficient of expansion as for the lower temperatures, and the value calculated for 1500°K is used for all temperatures above 900°K since the change in length at the different temperatures is very small.

On the high frequency side of the CO_2 bands an increase in temperature, at constant pressure, results in a decrease in emissivity, while on the low frequency side an increase in temperature causes an increase in emissivity. Under most conditions and at most frequencies, a 1 percent error in temperature would probably cause less than 1 percent error in the measured value of emissivity, but on the extreme low frequency side the error in emissivity might be as large as 3 or 4 percent.

Further sampling error arises from impurities and from uncertainties in the mixing ratio of the gases. N_2O is the only impurity in the CO_2 and $CO_2 + N_2$ mixtures which absorbs infrared radiation in the regions of the CO_2 bands, but even the absorption by N_2O near 3700 cm^{-1} is very small for hot samples and can be accounted for without introducing significant error. The $CO_2 + N_2$ mixtures were obtained from a local gas supply company which claimed an accuracy

of ± 0.5 percent. Unfortunately, many of the emissivity measurements were made before it was discovered that the mixing ratios of the gases did not meet the specifications. The gases ordered were supposed to be 1/16, 1/8, and 1/2 CO_2, but were found to have the mixing ratios of 0.074, 0.145 and 0.53, respectively. The values were determined by carefully comparing the infrared absorption by the pre-mixed samples to that by samples mixed in the laboratory. Measurements were made with an absorption cell at room temperature. Repeated measurements made by using different mixing techniques indicated that the fractions of CO_2 quoted above are accurate to approximately ± 1 percent except for the most dilute mixture which may be in error by as much as ± 2 percent. The purity of the "pure" CO_2 and of the H_2O investigated was probably greater than 99 percent.

Further uncertainty in sampling is introduced by the small leakage past the windows of the cell. The small amount of sample gas present in the end sections of the furnace tends to give an emissivity reading which is too high, while the argon which has leaked into the sample cell tends to make the reading too low. It was found that the emissivity measurement was insensitive to change in sample and argon flow rates over a wide range, indicating that the flow was not too fast for the gas to heat to the proper temperature and yet it was sufficiently fast to provide flushing. As a result of these findings, along with the spectra obtained for the gases bled into the monitor cell, it was concluded that leakage could not give rise to more than ± 1 percent uncertainty in the measured values of emissivity.

Absorption by the small amount of CO_2 and H_2O which could not be flushed from the monochromator could give rise to a maximum error in emissivity of approximately 0.01 at the frequencies of maximum absorption in the background. The absorptance by the residual CO_2 and H_2O was greater than 0.02 or 0.03 in only a few cases. This absorption can be partially accounted for, so that the maximum error should not exceed that stated above.

Certain small errors are introduced by possible nonlinearity of the detector and amplifier and by scanning too fast for the recorder to respond completely to give an accurate reading. According to the instrument manufacturer's specifications, the maximum error in emissivity values caused by nonlinearity of the detector and amplifier should not exceed 0.005 for values of emissivity near 0.50 and should be even less for values nearer zero or unity. Error introduced by scanning too fast for the response of the amplifier should be negligible, except possibly for frequencies near a very steep slope on the spectrum,

such as occurs on the high frequency side of the CO_2 absorption in the 2350 cm^{-1} region. Maxima and minima on the recordings may tend to be slightly "rounded" and shifted toward the direction of scan, which in the present study is from high to low frequencies. Since considerable care was taken to determine the proper scanning speeds, which were varied from one portion of a spectrum to another, the maximum error in emissivity due to slow "dynamic response" should not exceed 0.01 at any frequency, and the average over a 5 cm^{-1} interval is considerably less.

The operator of the digital read-out machine can read the recordings with an uncertainty that corresponds to approximately $\pm$ 0.004 in emissivity. The machine program performs the calculations as if the curves were composed of straight lines between the points read, and the points were sufficiently close that this "assumption" should never produce errors greater than 0.001 in the calculated values of average emissivity for 5 cm^{-1} intervals which are tabulated in Sections 2 and 3. Any other errors due to the machine are negligible, except for mistakes in the input such as duplicate cards or cards which were punched wrongly. Output errors due to incorrect cards are usually obvious when the emissivity curves are plotted, and corrections can easily be made. However, it is possible that a few obscure errors still exist in the tables of Sections 3 and 4. If so, these errors would appear in a close comparison of the tables with emissivity curves.

Errors in the frequency calibration of the spectrometer, which are approximately $\pm$ 1 cm^{-1} near the 2350 cm^{-1} region and $\pm$ 2 cm^{-1} near 3700 cm^{-1}, tend to shift the spectra but do not change the structure. Of course, such errors in calibration can produce large errors in emissivity at a particular frequency measured on a steep slope of a spectrum, but the error introduced for a very wide interval or band is negligible.

Because of the many sources of errors and because some are important for some conditions and not for others, it is difficult to summarize the uncertainties of the results in a concise manner. But, for most cases, it is believed that the values of emissivity less than 0.10 are probably accurate to $\pm$ 0.01, while the uncertainty may be as large as $\pm$ 0.03 or 0.04 for values of emissivity greater than approximately 0.5. It should be noted that differences in emissivity between neighboring frequencies, which are much less than the stated values of uncertainty, can be detected. This is true because the accuracy of the "shape" of a spectrum is considerably better than the absolute accuracy of the measurement at a single frequency. Changes in emissivity as small as 0.001 or 0.002 can frequently be detected between neighboring points.

SECTION 3

RESULTS: EMISSION BY HOT CO_2

This section contains the results of emission data obtained for more than 60 samples of CO_2 and $CO_2 + N_2$ at 1200°K and 1500°K. Mixtures of $CO_2 + N_2$ containing 7.4%, 14.5%, 53% and 100% of CO_2 were investigated at total pressures between approximately 6 and 1500 mm Hg. The length of the sample cell was 7.75 cm at the high temperatures. In general, the spectra were obtained in sets consisting of samples having a fixed temperature and fixed mixing ratio but at different total pressures. For a given sample the spectra of the 2350 cm^{-1} and the 3700 cm^{-1} regions were recorded separately. Several of the samples at lower pressures did not produce significant emission in the 3700 cm^{-1} region, and spectra were not scanned in this region. Although spectra were obtained in both regions for many of the samples, each spectrum has been given a different sample number for reference. Sample numbers for the 2350 cm^{-1} region are prefixed by the letter F, while those for the 3700 cm^{-1} region are prefixed by T.

Figures 3-1 through 3-8 show curves relating emissivity to frequency for the F-samples. The curves were replotted from the spectra obtained with spectral resolution given by schedule A in Table 2-1. Since loss of a little structure in the process of replotting is inevitable, all the emissivity curves shown in this report probably correspond to a spectral slit width 1 or 2 cm^{-1} wider than that shown in the corresponding resolution shcedule.

Emissivity curves for the T spectra (3700 cm^{-1}) region are shown in Figures 3-9 through 3-14. Resolution schedule C (Table 2-1) applies to the spectra from which these curves were obtained.

The growth of the emission with increasing pressure is seen to be quite large. It is well known[7] from similar studies of absorption by gases at lower temperatures that the growth observed by increasing the pressure of a given mixture is a result of both the increase in optical thickness and the increase in line width associated with higher pressure.

In Figure 3-15 are shown a set of curves relating $\int\epsilon(\nu)d\nu$ over the 2350 cm^{-1} region to total pressure for four different gas mixtures at $1200^{o}K$. The quantity $\int\epsilon(\nu)d\nu$ corresponds to the quantity $\int A(\nu)d\nu$ which is frequently used in absorption studies of gases because it is independent of the slit function under usual experimental conditions, provided the integration is carried out over the entire region of absorption. The features of the curves of Figure 3-15, which are drawn on log-log scales, are quite similar to curves of $\int A(\nu)d\nu$ for samples at room temperature which have been published.[7] The curves contain an almost straight portion and tend to level off at higher pressures as the emissivity approaches a maximum value of unity over much of the region, and the only growth occurs in the wings of the emitting region.

In order to demonstrate the effect of increasing pressure while maintaining constant optical thickness, points were read from the curves of Figure 3-15 and plotted in Figure 3-16, where each curve corresponds to a constant value of optical thickness. A rather small dependence on pressure is observed; the maximum slope of any of the curves is approximately 0.2, which indicates that the maximum dependence on pressure is $P^{0.2}$. It should be noted that the total pressure used in the abscissa of Figure 3-16 is due to $CO_2 + N_2$; and different points used in obtaining the curves represent samples having different ratios of the two gases. No attempt has been made to account for the different broadening abilities of the gases to obtain an equivalent pressure which is directly related to the widths of the spectral lines. The necessity of accounting for the different broadening abilities has been explained in considerable detail by Burch, Singleton, and Williams[8]. The curves of Figure 3-16 illustrate the effect of pressure broadening by an inert gas, N_2; but the dependence of emissivity on line width cannot be determined until measurements of the different broadening abilities have been made. Such measurements are planned in the near future as a part of the present investigation.

Information about each sample and about the measurements are given in considerable detail in Tables 3-1 and 3-2, covering the 2350 cm^{-1} and 3700 cm^{-1} regions, respectively. The tables were compiled by "stripping in" the output from the IBM computer for each sample; the tables were then photographed and reduced to page size.

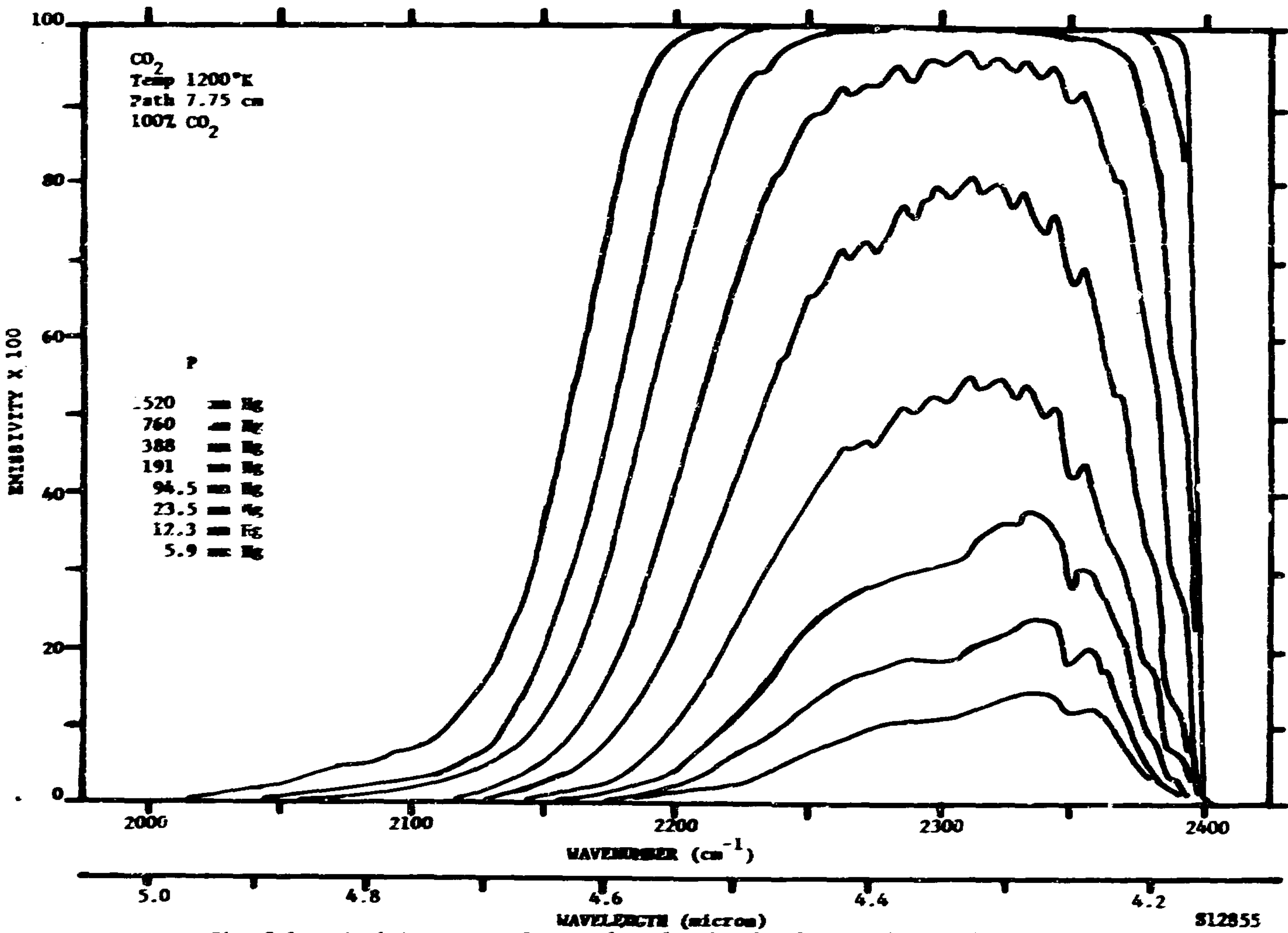

S12855

Fig. 3-1 Emissivity Curves for Samples F1, F2, F3, F4, F5, F6, F7, F8, and F9

WAVELENGTH (micron) S12855
Fig. 3-1 Emissivity Curves for Samples F1, F2, F3, F4, F5, F6, F7, F8, and F9

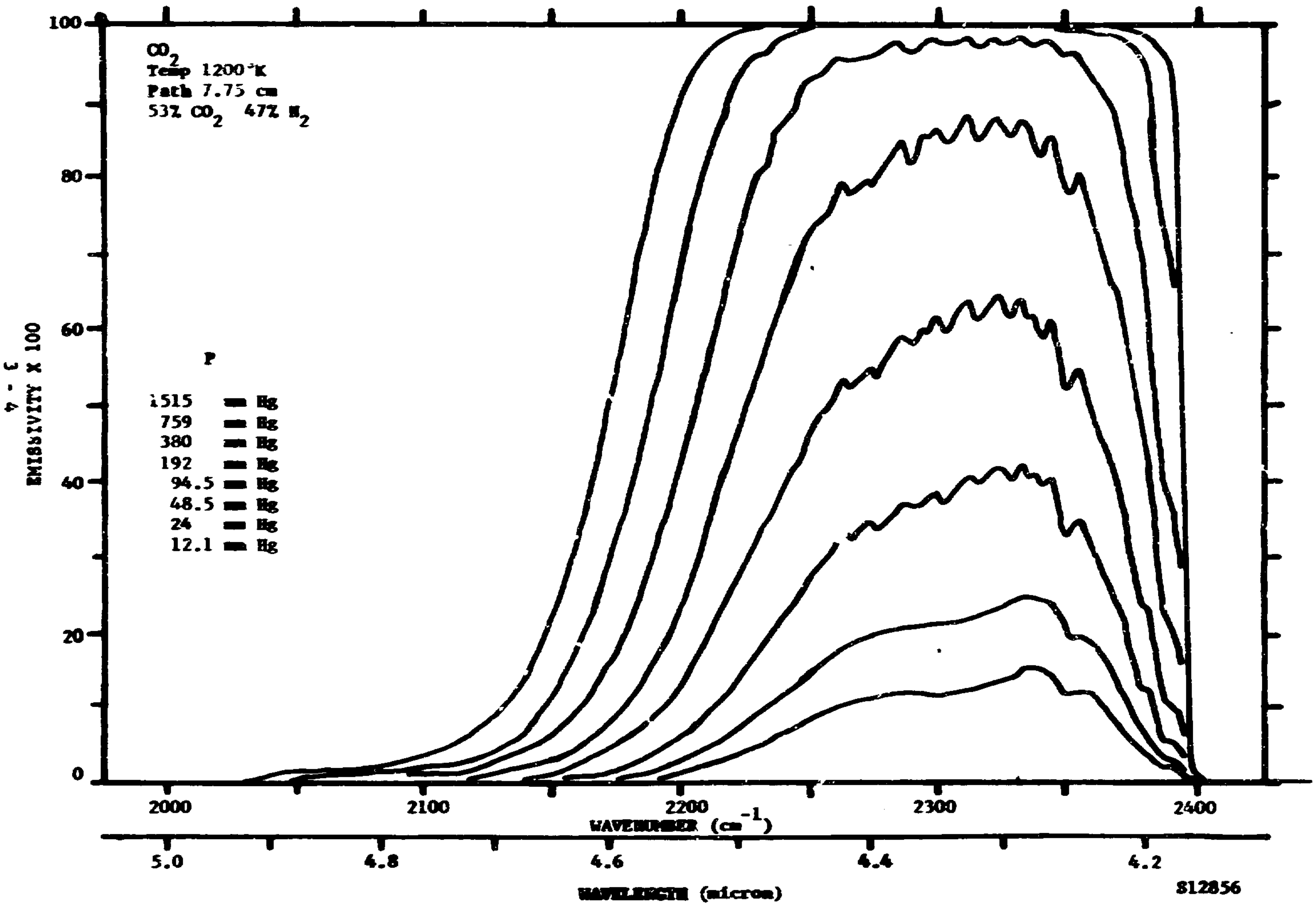

Fig. 3-2. Emissivity Curves for Samples F10, F11, F12, F13, F14, F15, F16, and F17

Fig. 3-2. Emissivity Curves for Samples F10, F11, F12, F13, F14, F15, F16, and F17

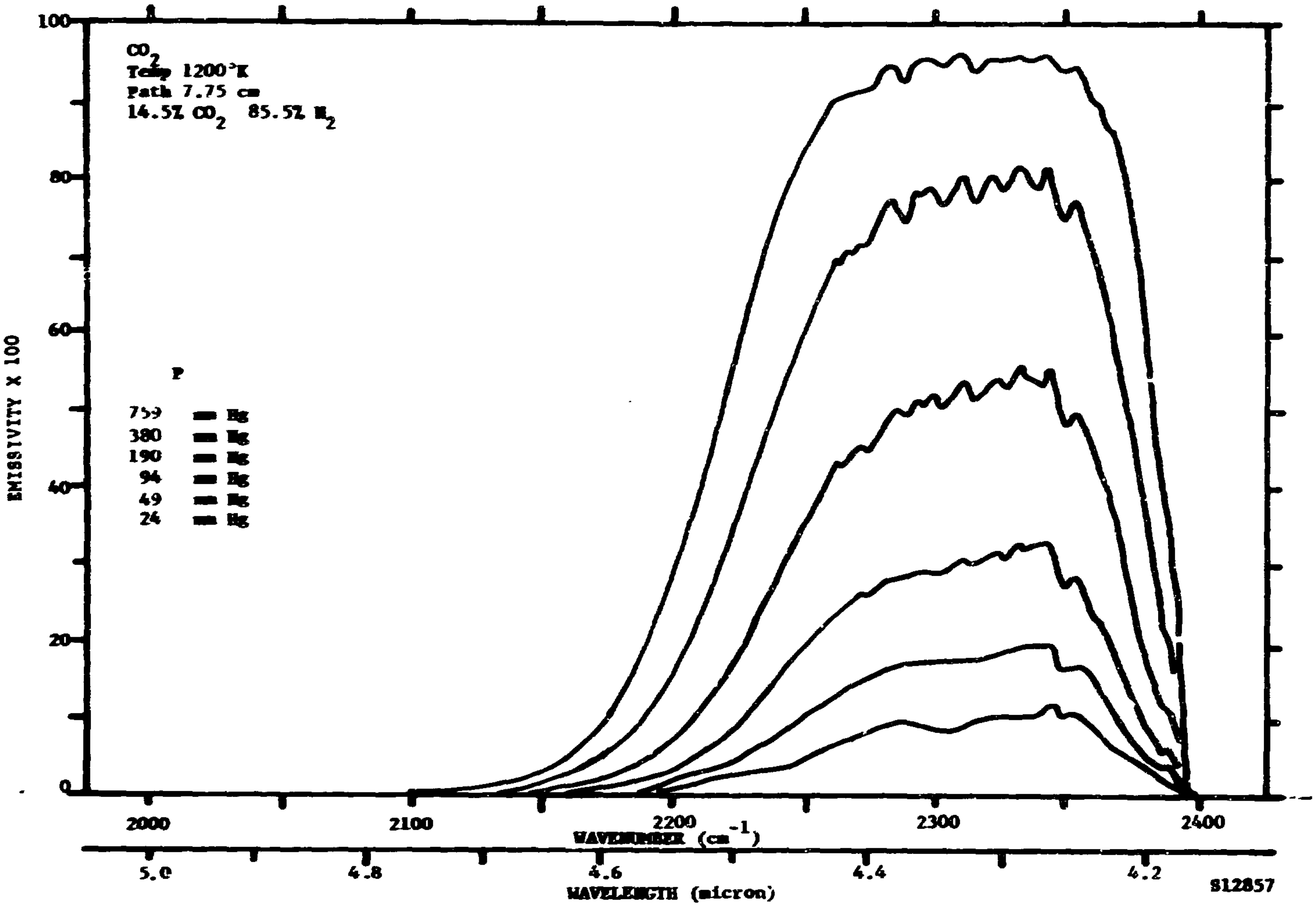

Fig. 3-3. Emissivity Curves for Samples F18, F19, F20, F21, F22, and F23

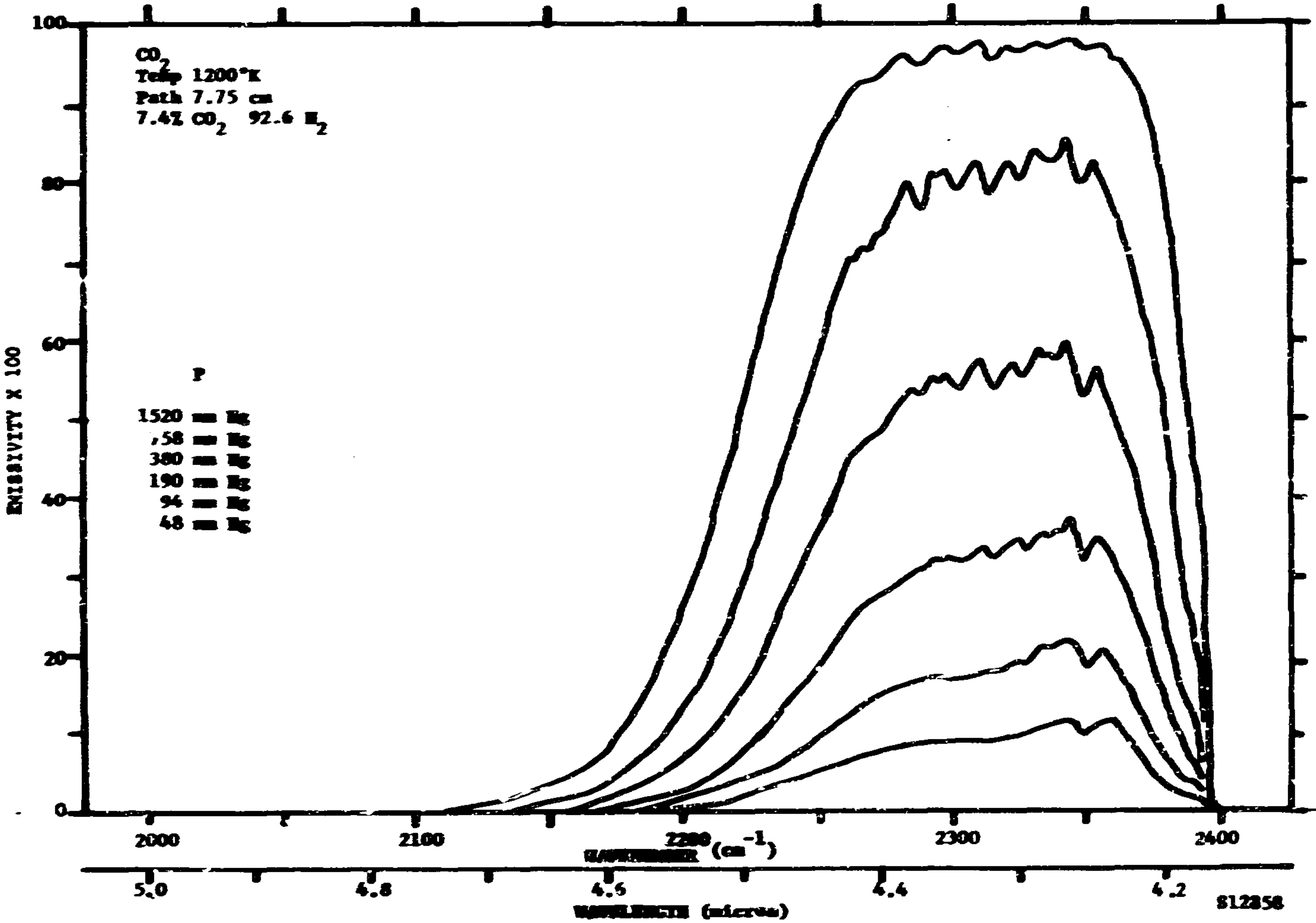

Fig. 3-4. Emissivity Curves for Samples F24, F25, F26, F27, F28, and F29

Fig. 3-4. Emissivity Curves for Samples F24, F25, F26, F27, F28, and F29

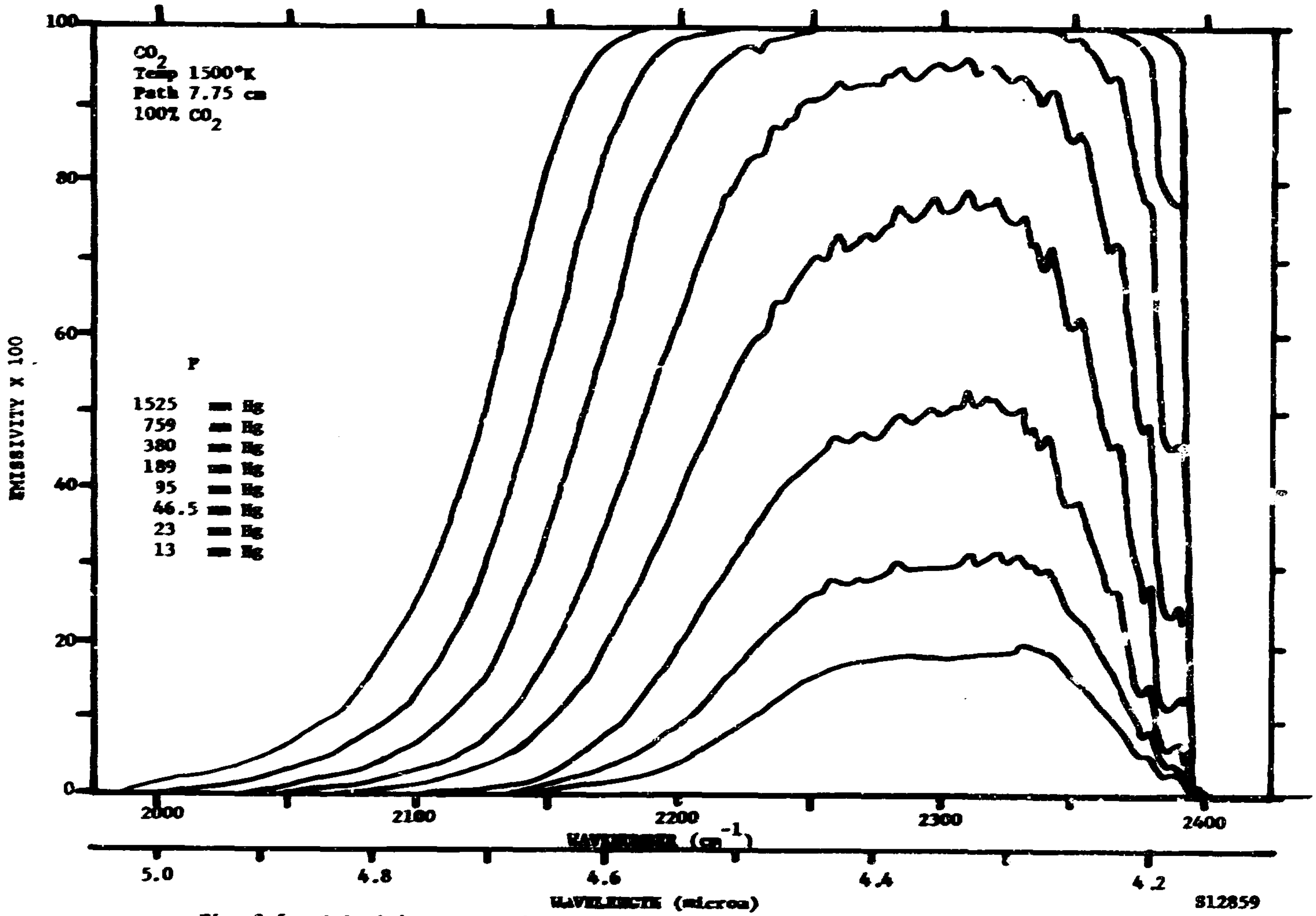

Fig. 3-5. Emissivity Curves for Samples F30, F31, F32, F33, F34, F35, F36, and F37

WAVELENGTH (micron)
Fig. 3-5. Emissivity Curves for Samples F30, F31, F32, F33, F34, F35, F36, and F37

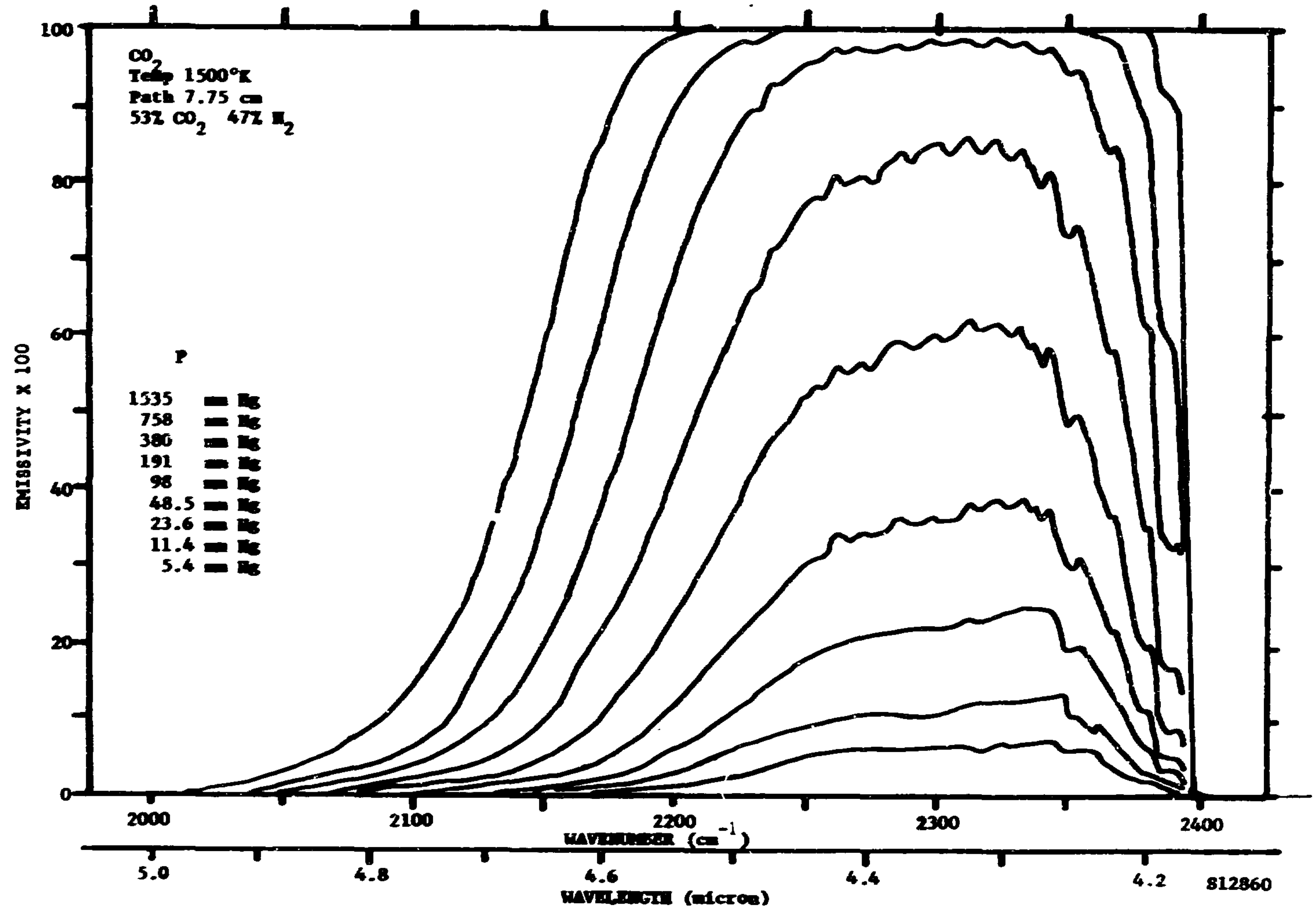

Fig. 3-6 Emissivity Curves for Samples F38, F39, F40, F41, F42, F43, F44, F45, and F46

Fig. 3-6 Emissivity Curves for Samples F38, F39, F40, F41, F42, F43, F44, F45, and F46

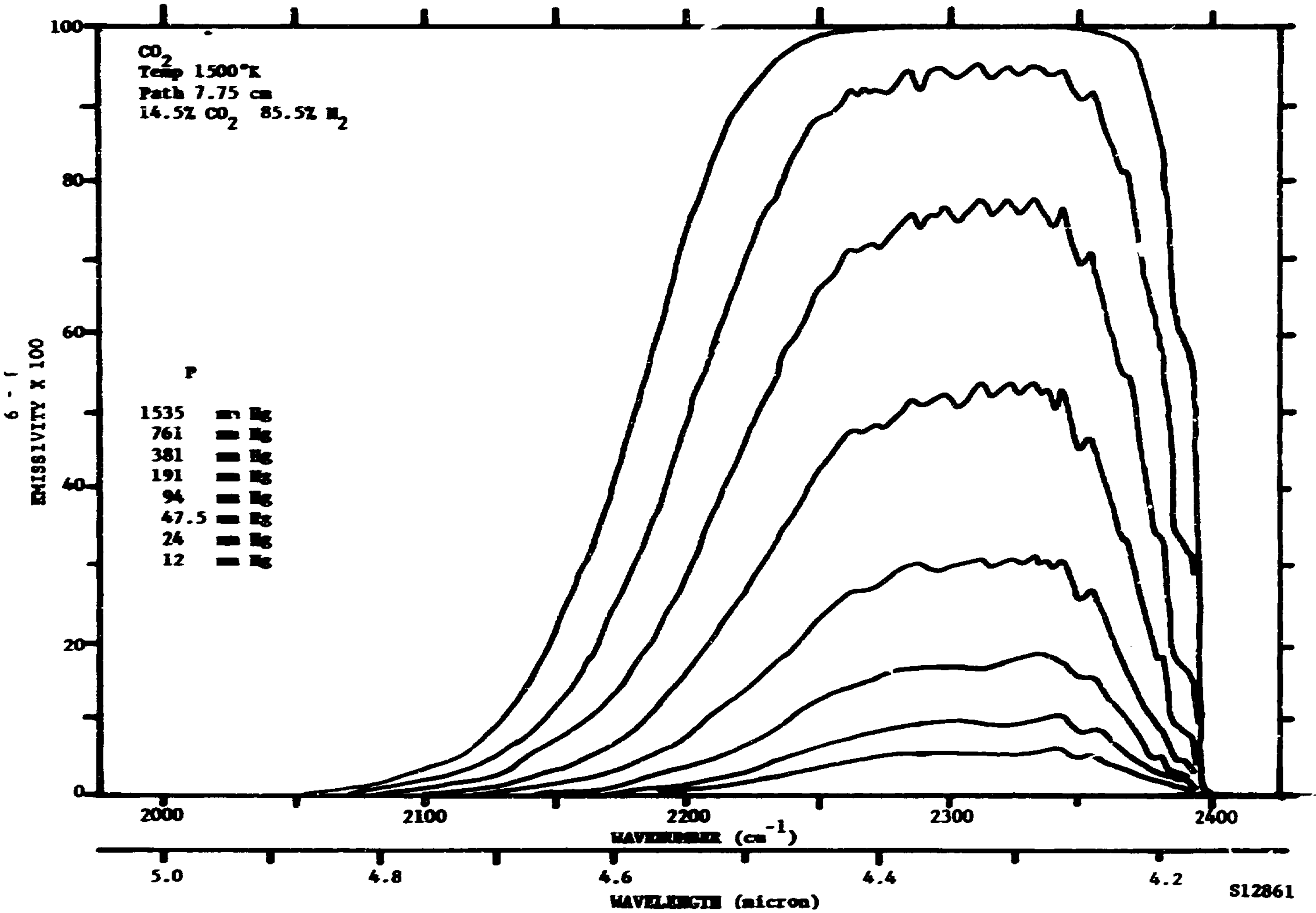

Fig. 3-7 Emissivity Curves for Samples F47, F48, F49, F50, F51, F52, F53, and F54

Fig. 3-7 Emissivity Curves for Samples F47, F48, F49, F50, F51, F52, F53, and F54

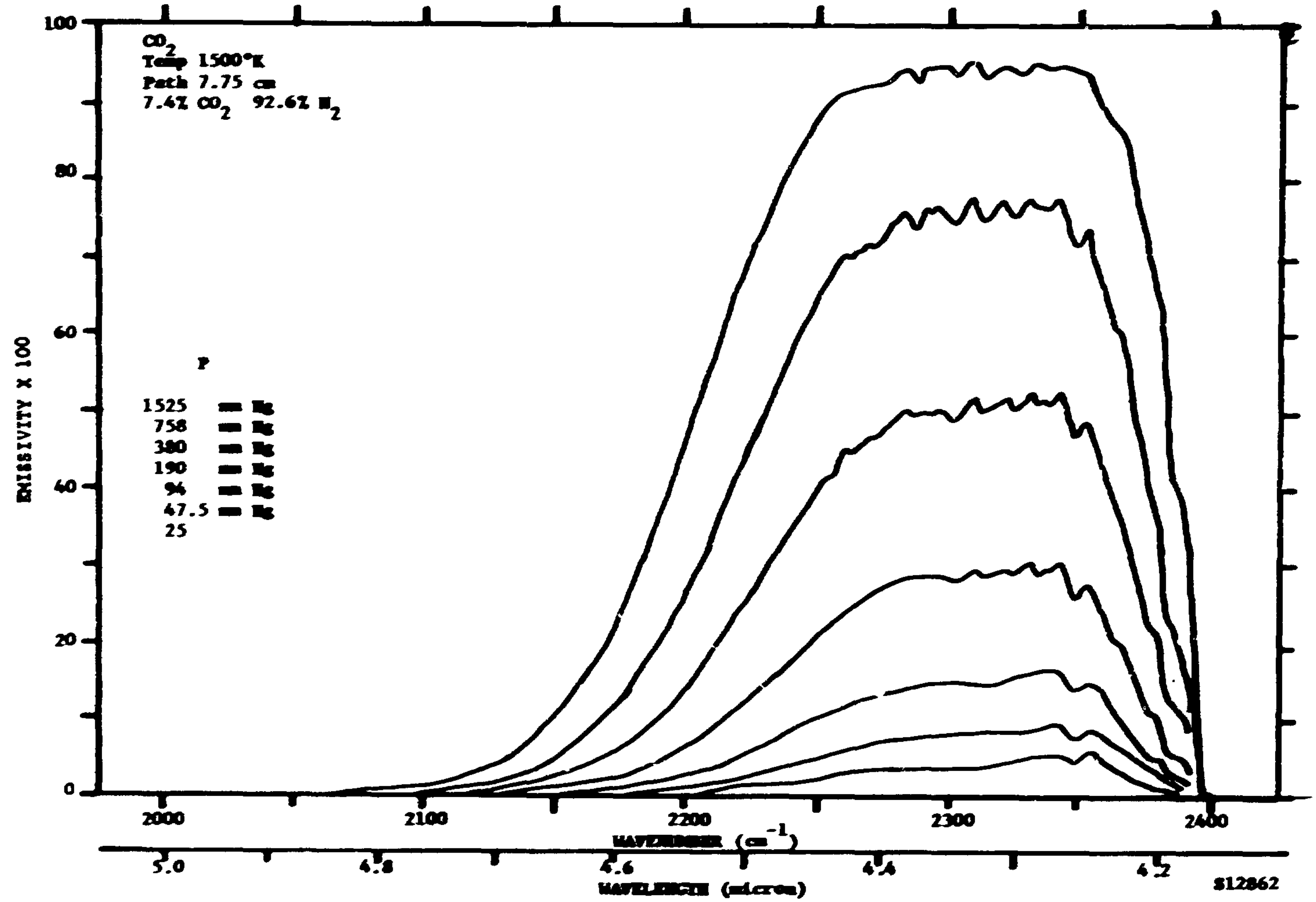

Fig. 3-8 Emissivity Curves for Samples F55, F56, F57, F58, F59, F60, and F61

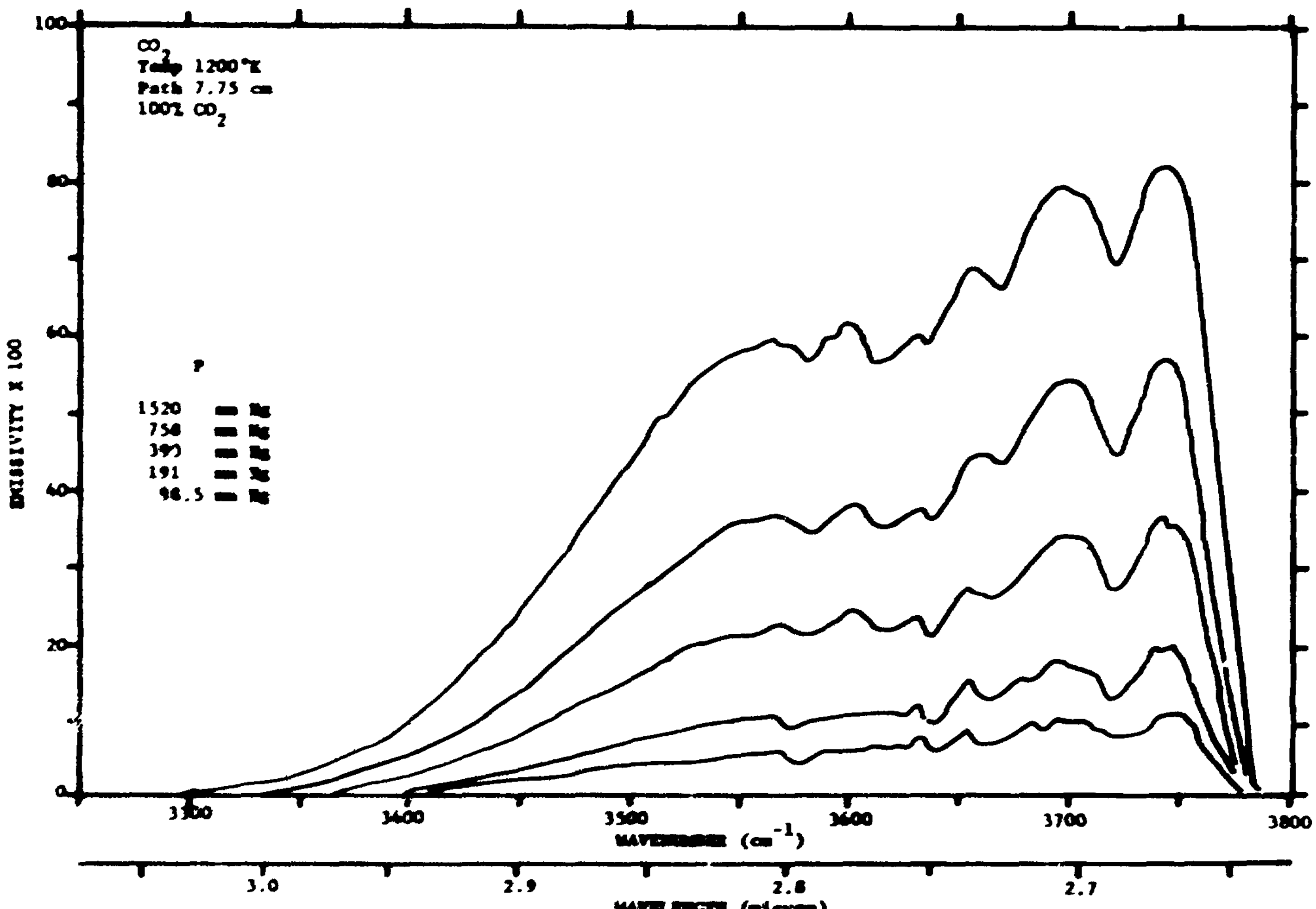

Fig. 3-9. Emissivity Curves for Samples T1, T2, T3. T4, and T5

812863

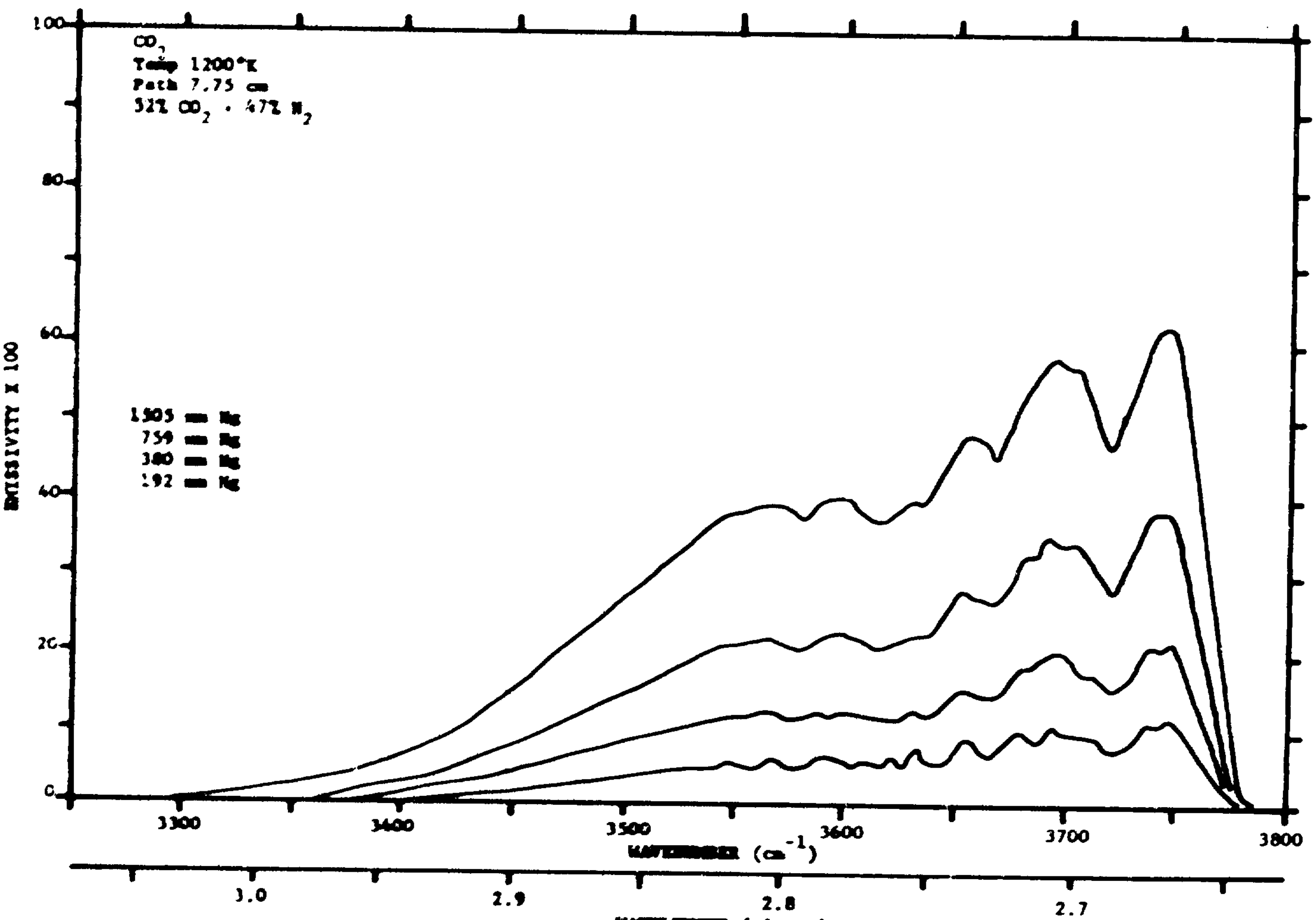

Fig. 3-10. Emissivity Curves for Samples T6, T7, T8, and T9

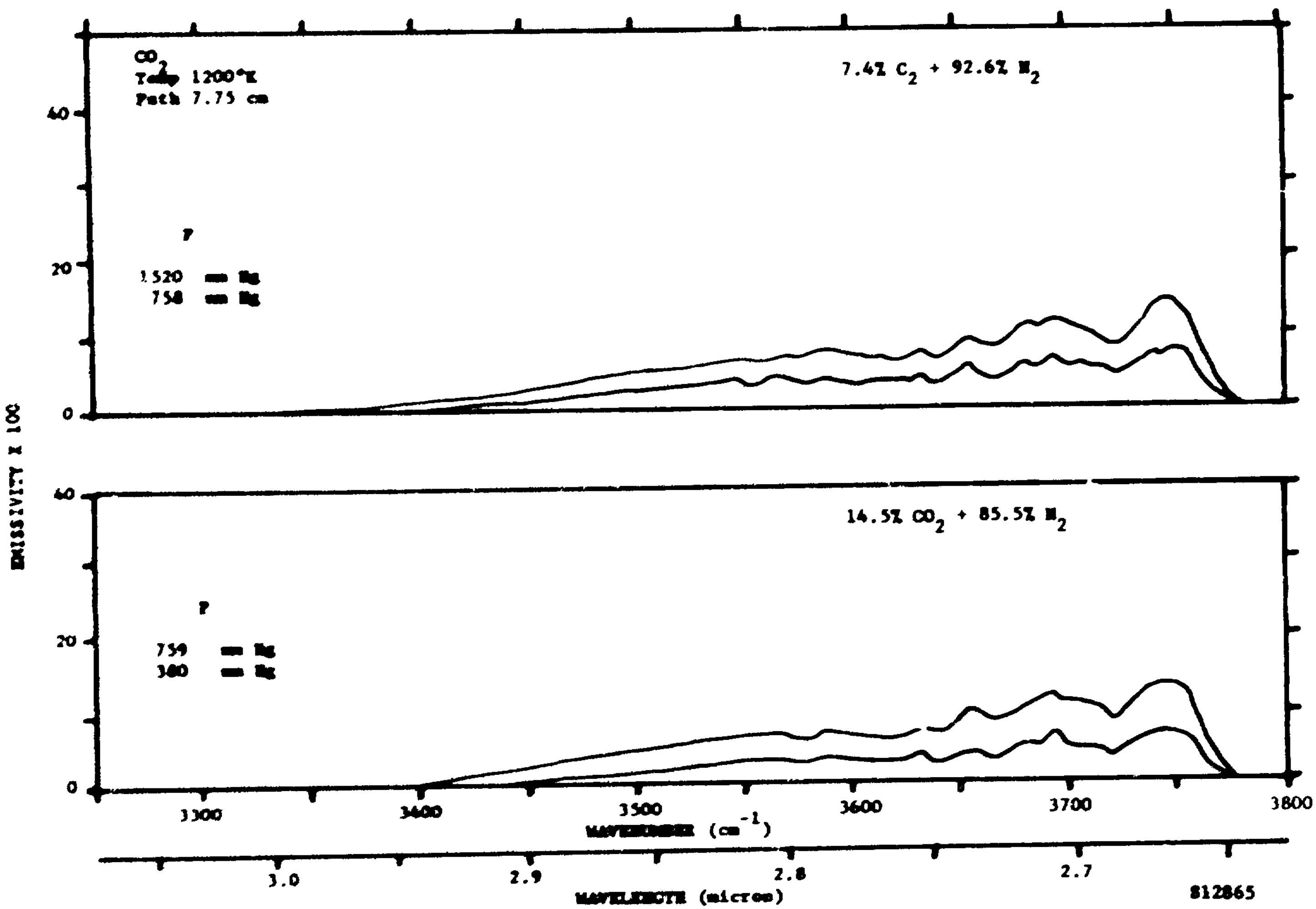

Fig. 3-11. Emissivity Curves for Samples T10, T11, T12, and T13

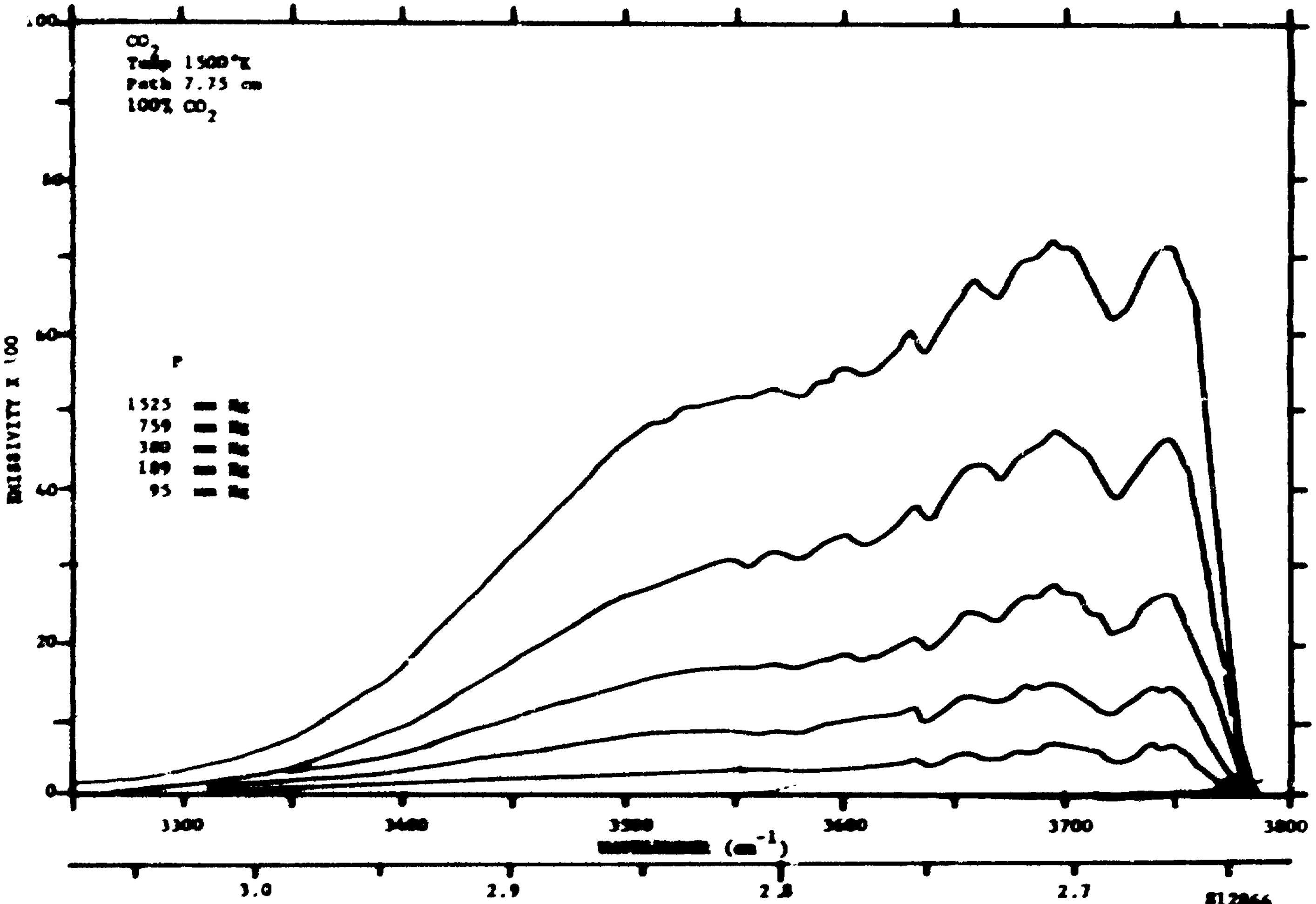

Fig. 3-12. Emissivity Curves for Samples T14, T15, T16, T17, and T18

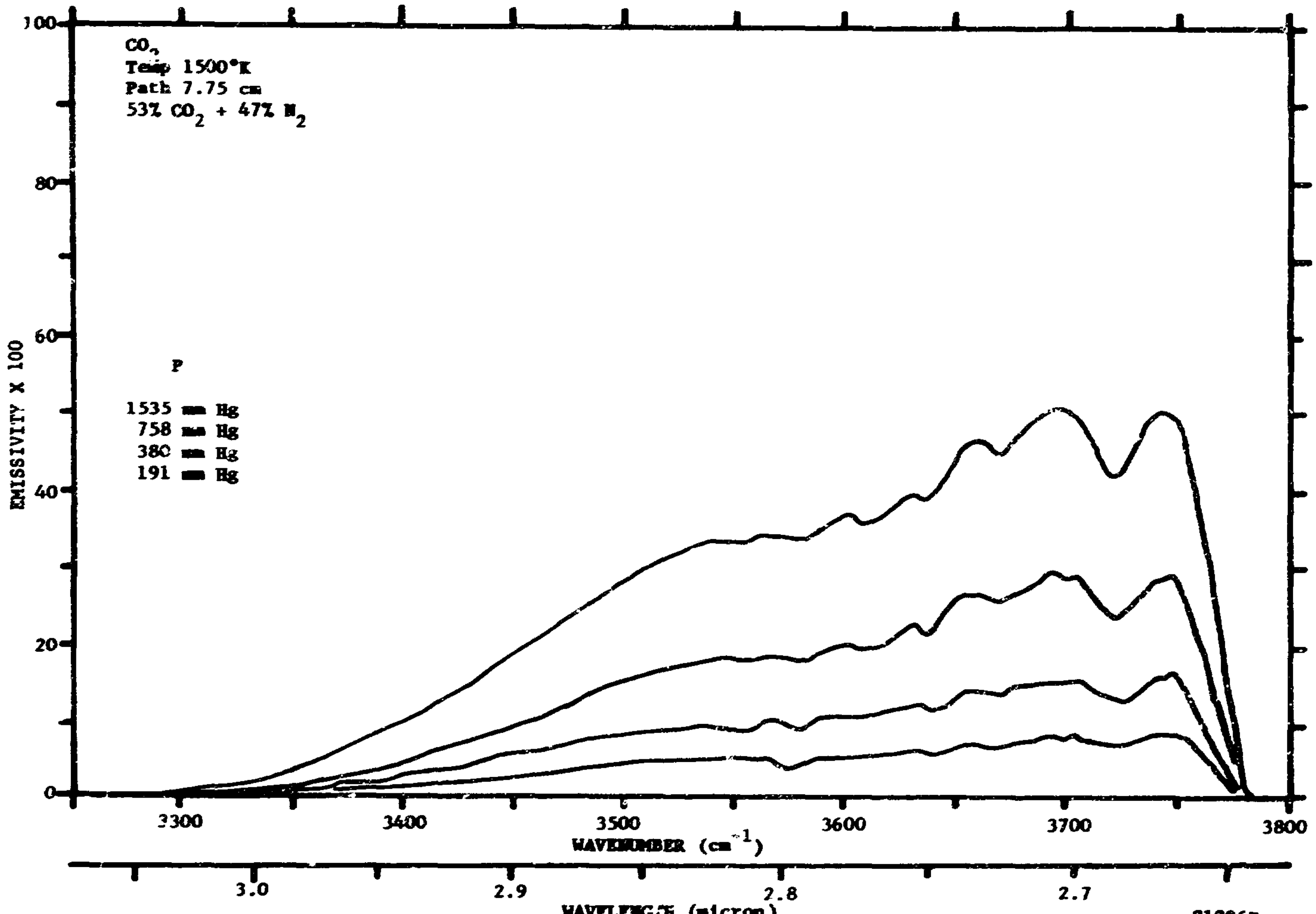

Fig. 3-13. Emissivity Curves for Samples T19, T20, T21, and T22

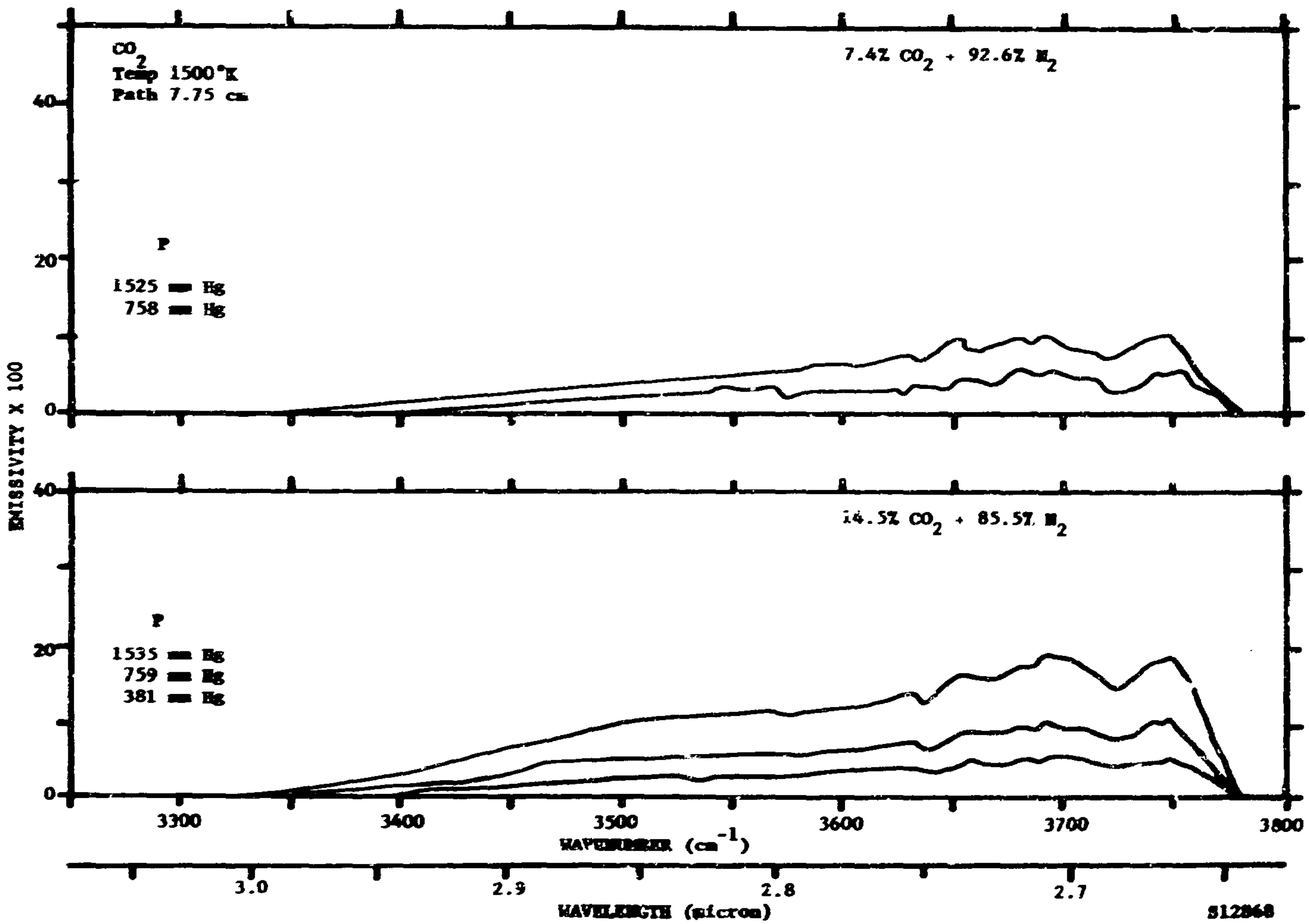

Fig. 3-14. Emissivity Curves for Samples T23, T24, T25, T26, and T27

Fig. 3-14. Emissivity Curves for Samples T23, T24, T25, T26, and T27

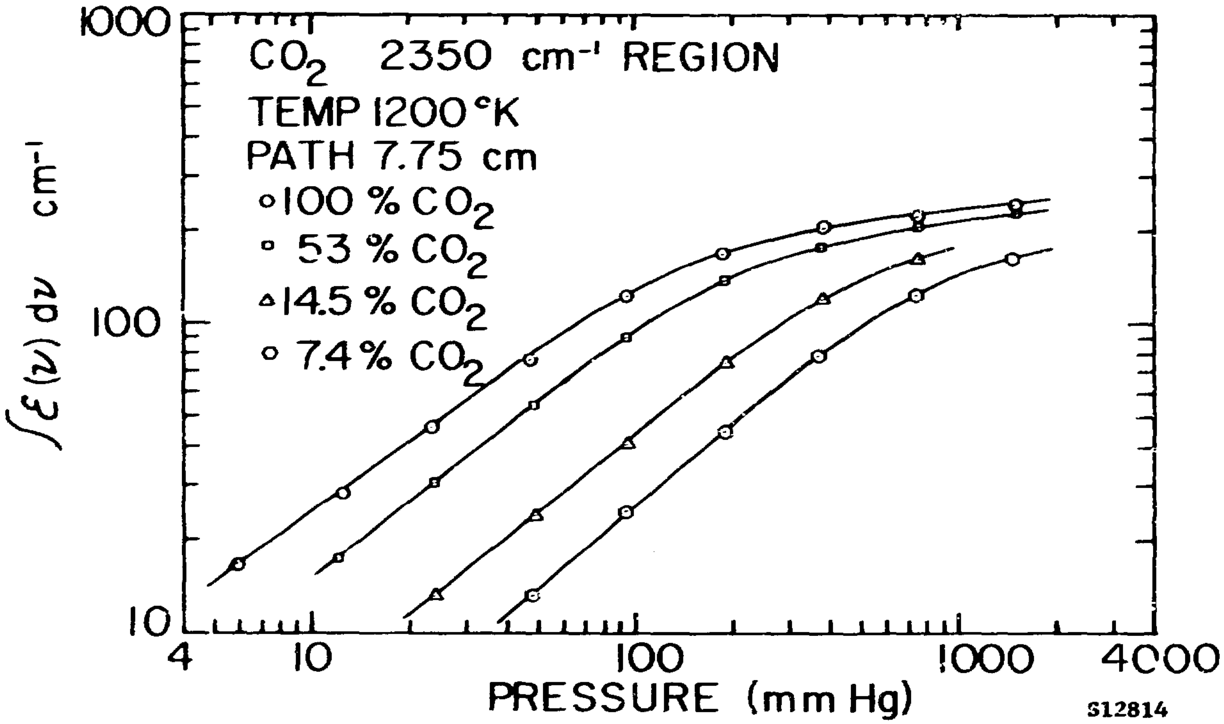

FIGURE 3-15. $\int \epsilon(\nu)\, d\nu$ FOR THE 2350 CM^{-1} REGION VERSUS THE TOTAL PRESSURE FOR SAMPLES HAVING CONSTANT MIXING RATIO

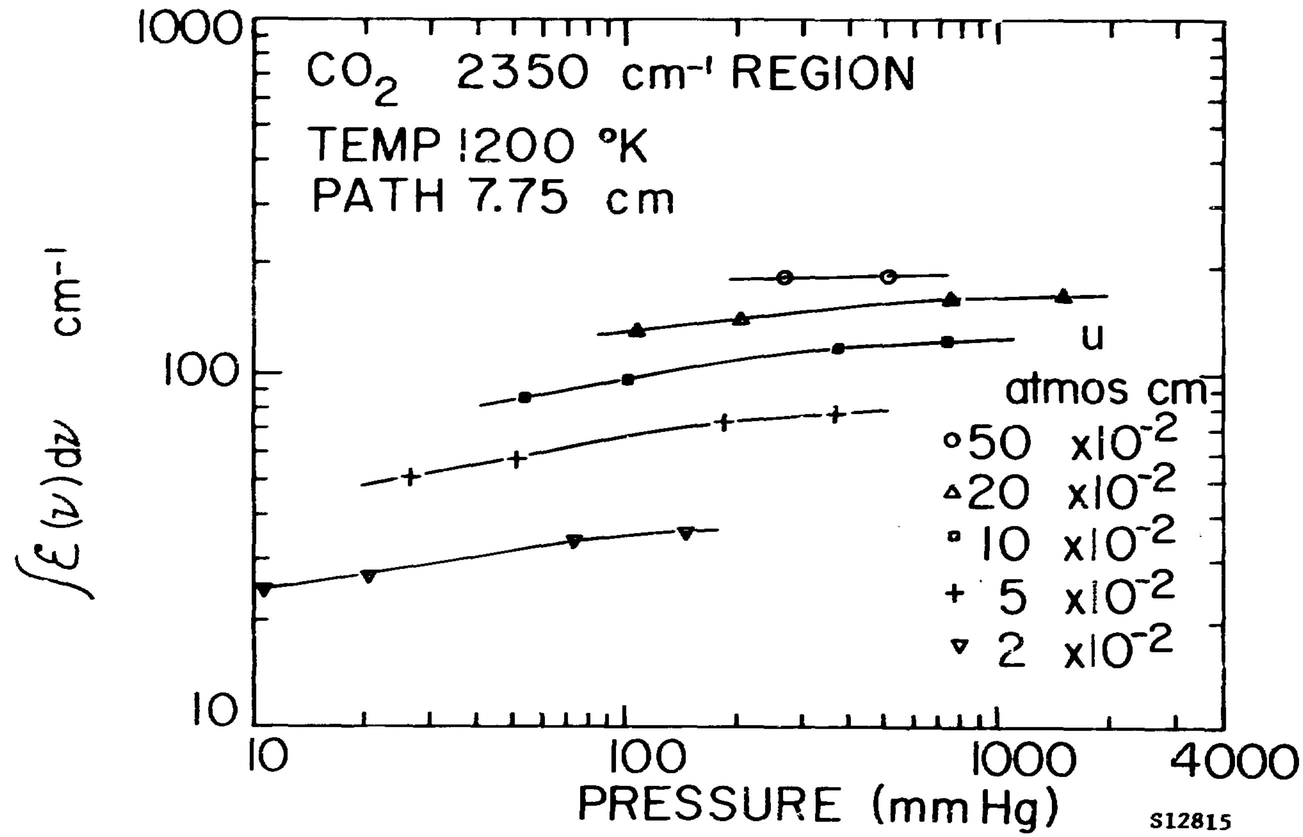

FIGURE 3-16. $\int \epsilon(\nu)\, d\nu$ FOR THE 2350 CM^{-1} REGION VERSUS THE TOTAL PRESSURE FOR SAMPLES HAVING CONSTANT VALUES OF OPTICAL THICKNESS

INFORMATION FOR USAGE OF TABLES 3-1 AND 3-2

Tables 3-1 and 3-2 have been divided into portions 3-1A, 3-1B, etc., since the information for all the samples included in each table could not be put on a single page. For example, 3-1A covers samples F1 through F7; 3-1B covers F8 through F14, etc. Tables 3-1A, 3-1B, etc. are each on one page, while 3-2A, 3-2B, and 3-2C are each two pages long.

The following information regarding each sample is given at the top of each table: The number assigned to each sample, the temperature, total pressure, ratio of the partial pressure of CO_2 to the total pressure, the optical thickness u, in atmos cm STP, $\int \epsilon(\nu) d\nu$ over the entire region of absorption, and the number of the figure containing the emissivity curve.

The interval is given in cm^{-1} in the first column and in microns in the second column. The third and fourth columns apply to sample F1, the fifth and sixth to F2, etc. In the left-hand column under each sample is given $\bar{\epsilon}$, the average value of emissivity over the interval; the right-hand column under each sample gives the radiance N over the interval in watts cm^{-2} steradian^{-1}. The multiplication factors 100 and 10,000 at the top of the columns should be noted.

The first portion of each table is devoted to intervals 50 cm^{-1} wide; and the remainder is for intervals 5 cm^{-1} wide. Radiance values for each 5 cm^{-1} interval are found by multiplying 5 times the average emissivity over the interval by $N^B(\nu_o)$, the spectral radiance at the center of the interval of a blackbody at the temperature of the gas. $N^B(\nu)$, the spectral radiance of a blackbody at frequency $\nu(cm^{-1})$ at temperature θ is given by:

$$N^B(\nu) = 1.1906 \times 10^{-12} \nu^3 \left\{ \exp\left[1.43868 \frac{\nu}{\theta}\right] - 1 \right\}^{-1} \qquad (3\text{-}1)$$

The power radiated from a 1 cm^2 surface of the gas sample in the frequency interval involved, through a small solid angle ω in a direction perpendicular to the surface, is given by ωN. The requirement for the power to equal ωN is that the cosine of the angle between the surface and any of the rays in the beam be approximately equal to unity.

The total power radiated in a hemisphere from a 1 cm^2 flat surface of a blackbody is given by $\pi N^B(\nu)$.

Values of N for the 50 cm^{-1} intervals were found by summing the values for the ten 5 cm^{-1} intervals included; values of $\bar{\epsilon}$ for 50 cm^{-1} intervals were found by taking one-tenth the sum of the values of $\bar{\epsilon}$ for the ten 5 cm^{-1} intervals.

Although the output of the computer included two figures after the decimal point in the $\bar{\epsilon}$ columns and three figures after the decimal point in the N column, the last figure in each of the columns should not be considered significant. Uncertainties in the tabulated values are discussed in Section 2.

TABLE 3-1A

Sample No.	P1	P2	P3	P4	P5	P6	P7
Temp. (°K)	1400°K	1400°K	1400°K	1400°K	1400°K	1400°K	1400°K
P (mm Hg)	[illegible]	[illegible]	[illegible]	[illegible]	[illegible]	[illegible]	[illegible]
p CO/P	100%	100%	100%	100%	100%	100%	100%
u (atm-cm STP)	[illegible]	[illegible]	[illegible]	[illegible]	[illegible]	[illegible]	[illegible]
Fig. No.	[illegible]	[illegible]	[illegible]	[illegible]	[illegible]	[illegible]	[illegible]

Interval cm⁻¹	Interval microns	Ā × 100	N × 10,000	Ā × 100	N × 10,000	Ā × 100	N × 10,000	Ā × 100	N × 10,000	Ā × 100	N × 10,000	Ā × 100	N × 10,000	Ā × 100	N × 10,000
[illegible]	[illegible]	[illegible]	[illegible]	[illegible]	[illegible]	[illegible]	[illegible]	[illegible]	[illegible]	[illegible]	[illegible]	[illegible]	[illegible]	[illegible]	[illegible]

TABLE 3-18

Sample No. / Temp. (°K) / P (atm Hg) / p (CO₂)/P / u (atm-cm STP) / Δ(1/λ) (cm⁻¹) / Fig. No.		P8		P9		P10		P11		P12		P13		P14	
		1800°K		1800°K		1800°K		1800°K		1800°K		1800°K		1800°K	
Interval cm⁻¹	microns	ε̄ × 100	N × 10,000	ε̄ × 100	N × 10,000	ε̄ × 100	N × 10,000	ε̄ × 100	N × 10,000	ε̄ × 100	N × 10,000	ε̄ × 100	N × 10,000	ε̄ × 100	N × 10,000
1950-2000	5.1282-5.0000	0.	0.	0.	0.	0.	0.	0.	0.	0.	0.	0.	0.	0.	0.
2000-2050	5.0000-4.8780	[illegible]	[illegible]	1.00	[illegible]	0.	0.	0.	0.	0.	0.	0.	0.	0.	0.
2050-2100	4.8780-4.7619	2.11	[illegible]	[illegible]	[illegible]	0.	[illegible]	0.	0.	0.	0.	0.	0.	[illegible]	[illegible]
2100-2150	4.7619-4.6512	[illegible]	[illegible]	[illegible]	[illegible]	0.	[illegible]	0.	0.	[illegible]	[illegible]	[illegible]	[illegible]	[illegible]	[illegible]
2150-2200	4.6512-4.5455	[illegible]	[illegible]	[illegible]	[illegible]	[illegible]	[illegible]	[illegible]	[illegible]	[illegible]	[illegible]	[illegible]	[illegible]	[illegible]	[illegible]
2200-2250	4.5455-4.4444	[illegible]	[illegible]	[illegible]	[illegible]	[illegible]	[illegible]	[illegible]	[illegible]	[illegible]	[illegible]	[illegible]	[illegible]	[illegible]	[illegible]
2250-2300	4.4444-4.3478	100.00	[illegible]	100.00	[illegible]	[illegible]	[illegible]	[illegible]	[illegible]	[illegible]	[illegible]	[illegible]	[illegible]	[illegible]	[illegible]
2300-2350	4.3478-4.2553	100.00	[illegible]	100.00	[illegible]	[illegible]	[illegible]	[illegible]	[illegible]	[illegible]	[illegible]	[illegible]	[illegible]	[illegible]	[illegible]
2350-2400	4.2553-4.1667	[illegible]	[illegible]	[illegible]	[illegible]	[illegible]	[illegible]	[illegible]	[illegible]	[illegible]	[illegible]	[illegible]	[illegible]	[illegible]	[illegible]

TABLE 3-1C

Sample No.		F15		F16		F17		F18		F19		F20		F21	
Temp (°K)		1200°K		1200°K		1200°K		1200°K		1200°K		1200°K		1200°K	
P (mm Hg)		180		749		1519		24		49		94		190	
$p(CO_2)/P$		51%		51%		51%		16.5%		16.5%		16.5%		16.5%	
u (atm-cm STP)		471×10^{-1}		940×10^{-1}		1880×10^{-1}		8.14×10^{-1}		16.6×10^{-1}		11.8×10^{-1}		64.1×10^{-1}	
$\int \epsilon\, d\omega$ (cm^{-1})		179		208		228		13.1		21.5		41.4		74.5	
Fig. No.		1-2		1-2		1-2		1-1		1-1		1-1		1-1	
Interval cm^{-1}	microns	ϵ × 100	N × 10,000	ϵ × 100	N × 10,000	ϵ × 100	N × 10,000	ϵ × 100	N × 10,000	ϵ × 100	N × 10,000	ϵ × 100	N × 10,000	ϵ × 100	N × 10,000
1950-2000	5.1282-5.0000	0.	0.	0	0.	0.	0.	0.	0.	0.	0.	0.	0.	0.	0.
2000-2050	5.0000-4.8780	0.01	0.027	0.22	0.372	0.46	2.210	0.	0.	0.	0.	0.	0.	0.	0.
2050-2100	4.8780-4.7619	0.96	4.556	1.46	7.046	2.32	11.160	0.	0.	0.	0.	0.	0.	0.	0.
2100-2150	4.7619-4.6512	4.05	14.662	3.00	14.248	9.99	48.492	0.	0.	0.	0	0.00	0.001	0.11	0.560
2150-2200	4.6512-4.5455	20.80	101.405	36.11	178.061	56.02	271.102	0.10	0.516	0.41	2.088	1.30	6.552	3.06	14.830
2200-2250	4.5455-4.4444	77.49	356.595	91.05	445.201	98.51	480.815	2.76	13.511	5.19	25.600	10.19	49.866	19.63	96.030
2250-2300	4.4444-4.3478	96.17	472.610	100.00	490.176	100.00	490.176	7.93	38.896	16.07	78.904	35.80	176.467	45.60	223.556
2300-2350	4.3478-4.2553	91.91	440.552	99.45	490.689	100.00	490.766	10.06	48.556	18.22	89.176	30.98	152.062	53.10	260.627
2350-2400	4.2553-4.1667	66.15	327.665	82.66	405.610	88.11	431.506	5.19	25.136	8.67	42.566	15.77	78.512	32.75	156.173
2025-2030	4.9383-4.9261	-0.	0.	0.00	0.000	0.06	0.020	-0.	-0.	-0.	-0.	-0.	-0.	-0.	-0.
2030-2035	4.9261-4.9140	-0.	-0.	0.00	0.000	0.46	0.220	-0.	-0.	-0.	-0.	-0.	-0.	-0.	-0.
2035-2040	4.9140-4.9020	-0.	-0.	0.08	0.018	1.01	0.486	-0.	-0.	-0.	-0.	-0.	-0.	-0.	-0.
2040-2045	4.9020-4.8900	0.	0.	0.15	0.167	1.49	0.715	-0.	0.	-0.	-0.	-0.	-0.	-0.	-0.
2045-2050	4.8900-4.8780	0.06	0.027	0.19	0.177	1.60	0.769	-0.	-0.	-0.	-0.	-0.	-0.	-0.	-0.
[illegible]	[illegible]	[illegible]	[illegible]	[illegible]	[illegible]	[illegible]	[illegible]	[illegible]	[illegible]	[illegible]	[illegible]	[illegible]	[illegible]	[illegible]	[illegible]
[illegible]	[illegible]	[illegible]	[illegible]	[illegible]	[illegible]	[illegible]	[illegible]	[illegible]	[illegible]	[illegible]	[illegible]	[illegible]	[illegible]	[illegible]	[illegible]
[illegible]	[illegible]	[illegible]	[illegible]	[illegible]	[illegible]	[illegible]	[illegible]	[illegible]	[illegible]	[illegible]	[illegible]	[illegible]	[illegible]	[illegible]	[illegible]
[illegible]	[illegible]	[illegible]	[illegible]	[illegible]	[illegible]	[illegible]	[illegible]	[illegible]	[illegible]	[illegible]	[illegible]	[illegible]	[illegible]	[illegible]	[illegible]
[illegible]	[illegible]	[illegible]	[illegible]	[illegible]	[illegible]	[illegible]	[illegible]	[illegible]	[illegible]	[illegible]	[illegible]	[illegible]	[illegible]	[illegible]	[illegible]

3-23

TABLE 3-1D

Sample No.		F23		F31		F24		F19		F28		F27		F40	
Temp. (°K)		1200°K		1200°K		1200°K		1200°K		1200°K		1200°K		1200°K	
P (mm Hg)		300		739		40		94		190		380		750	
$p(CO_2)/P$		14.5%		14.5%		7.6%		7.4%		7.4%		7.4%		7.4%	
u (atm cm STP)		129×10^{-3}		250×10^{-3}		8.89×10^{-3}		16.2×10^{-3}		32.8×10^{-3}		65.7×10^{-3}		131×10^{-3}	
$\int k\, d\nu$ (cm^{-1})		121		162		13.0		24.5		44.9		78.9		127	
Fig. No.		3-3		3-3		3-4		3-4		3-4		3-4		3-4	
Interval cm^{-1}	microns	$\bar{\epsilon}_\pi$ 100	N × 10,000	$\bar{\epsilon}_\pi$ 100	N × 10,000	$\bar{\epsilon}_\pi$ 100	N × 10,000	$\bar{\epsilon}_\pi$ 100	N × 10,000	$\bar{\epsilon}_\pi$ 100	N × 10,000	$\bar{\epsilon}_\pi$ 100	N × 10,000	$\bar{\epsilon}_\pi$ 100	N × 10,000
1950-2000	5.1282-5.0000	0.	0.	0.	0.	0.	0.	0.	0.	0.	0.	0.	0.	0.	0.
2000-2050	5.0000-4.8780	0.	0.	0.	0.	0.	0.	0.	0.	0.	0.	0.	0.	0.	0.
2050-2100	4.8780-4.7619	0.01	0.035	0.09	0.450	0.	0.	0.	0.	0.	0.	0.	0.	0.	0.
2100-2150	4.7619-4.6512	1.25	6.073	1.45	7.020	0.	0.	0.	0.	0.	0.	0.	0.	0.35	1.615
2150-2200	4.6512-4.5455	7.03	34.101	12.47	60.015	0.03	0.125	0.36	1.645	1.02	4.965	2.61	12.761	5.05	20.419
2200-2250	4.5455-4.4444	36.70	179.944	57.15	279.365	2.65	12.883	5.16	25.102	9.97	48.741	19.27	94.270	33.96	166.105
2250-2300	4.4444-4.3478	72.18	351.076	92.02	451.120	7.66	37.452	14.53	71.223	27.47	134.652	48.55	238.042	73.56	360.634
2300-2350	4.3478-4.2553	79.36	389.338	95.75	469.900	9.85	48.369	18.75	92.090	33.77	165.525	56.24	276.025	81.70	401.005
2350-2400	4.2553-4.1667	46.20	226.883	65.37	320.871	5.07	24.849	10.41	51.100	18.71	91.822	31.20	153.616	51.76	254.071
2075-2080	4.8193-4.8077	-0.	-0.	0.	0.	-0.	-0.	-0.	-0.	-0.	-0.	-0.	-0.	-0.	-0.
2080-2085	4.8077-4.7962	-0.	-0.	0.03	0.015	-0.	-0.	-0.	-0.	-0.	-0.	-0.	-0.	-0.	-0.
2085-2090	4.7962-4.7847	-0.	-0.	0.16	0.077	-0.	-0.	-0.	-0.	-0.	-0.	-0.	-0.	-0.	-0.
2090-2095	4.7847-4.7733	0.	0.	0.30	0.149	-0.	-0.	-0.	-0.	-0.	-0.	-0.	-0.	-0.	-0.
2095-2100	4.7733-4.7619	0.07	0.035	0.44	0.218	-0.	-0.	-0.	-0.	-0.	-0.	-0.	-0.	-0.	-0.
2100-2105	4.7619-4.7506	0.38	0.186	0.58	0.288	-0.	-0.	-0.	-0.	-0.	-0.	-0.	-0.	-0.	-0.
2105-2110	4.7506-4.7393	0.53	0.258	0.71	0.346	-0.	-0.	-0.	-0.	-0.	-0.	-0.	-0.	-0.	-0.
2110-2115	4.7393-4.7281	0.75	0.361	0.85	0.412	-0.	-0.	-0.	-0.	-0.	-0.	-0.	-0.	-0.	-0.
[illegible]	[illegible]	[illegible]	[illegible]	[illegible]	[illegible]	[illegible]	[illegible]	[illegible]	[illegible]	[illegible]	[illegible]	[illegible]	[illegible]	[illegible]	[illegible]

TABLE 3-IE

Sample No.		F9		F10		F11		F12		F13		F14		F15	
Temp (°K)		1200°K		1500°K		1500°K		1500°K		1500°K		1500°K		1500°K	
P (mm Hg)		[illegible]		[illegible]		[illegible]		[illegible]		[illegible]		109		109	
p(CO)/P		[illegible]		100%		100%		100%		100%		100%		100%	
u (atm-cm STP)		[illegible] $\times 10^{-3}$		[illegible] $\times 10^{-3}$		[illegible] $\times 10^{-3}$		[illegible] $\times 10^{-3}$		[illegible] $\times 10^{-3}$		[illegible] $\times 10^{-3}$		717 $\times 10^{-3}$	
[illegible] (cm^{-1})		167		[illegible]		[illegible]		[illegible]		147		104		[illegible]	
Fig. No.		[illegible]		[illegible]		[illegible]		[illegible]		[illegible]		[illegible]		[illegible]	
Interval cm^{-1}	microns	$\bar{\alpha}$ x 100	N x 10,000	$\bar{\alpha}$ x 100	N x 10,000	$\bar{\alpha}$ x 100	N x 10,000	$\bar{\alpha}$ x 100	N x 10,000	$\bar{\alpha}$ x 100	N x 10,000	$\bar{\alpha}$ x 100	N x 10,000	$\bar{\alpha}$ x 100	N x 10,000
1950-2000	5.1282-5.0000	0.	0.	0.	0.	0.	0.	0.	0.	0.	0.	0.	0.	0.	0.

TABLE 3-1F

Sample No. / Temp (°K) / P (atm Hg) / p(CO)/P / u / Δν / Fig. No.	[illegible] 1500°K		[illegible] 1500°K		[illegible] 1500°K		[illegible] 1500°K		[illegible] 1500°K		[illegible] 1500°K		[illegible] 1500°K	
Interval cm^{-1} / microns	[illegible] 100	[illegible] 10,000	[illegible] 100	[illegible] 10,000	[illegible] 100	[illegible] 10,000	[illegible] 100	[illegible] 10,000	[illegible] 100	[illegible] 10,000	[illegible] 100	[illegible] 10,000	[illegible] 100	[illegible] 10,000
[illegible]	[illegible]	[illegible]	[illegible]	[illegible]	[illegible]	[illegible]	[illegible]	[illegible]	[illegible]	[illegible]	[illegible]	[illegible]	[illegible]	[illegible]

TABLE 3-1G

TABLE 3-1H

Sample No. / Temp. (°K) / P mm Hg / p(CO)/P / ω (atm cm STP) / ∫A(ν)dν (cm⁻²) / Fig. No.		F50 / 1500°K / 96 / 14.5% / 25.8 × 10⁻¹ / 66.9 / 3-7		F51 / 1500°K / 191 / 14.5% / 52.8 × 10⁻¹ / 81.5 / 3-7		F52 / 1500°K / 381 / 14.5% / 104 × 10⁻¹ / 1-8 / 3-7		F53 / 1500°K / 761 / 14.5% / 208 × 10⁻¹ / 176 / 3-7		F54 / 1500°K / 1518 / 14.5% / 421 × 10⁻¹ / 41? / 3-7		F55 / 1500°K / 25 / 7.6% / 1.90 × 10⁻¹ / 4.50 / 3-8		F56 / 1500°K / 67.1 / 7.6% / 6.64 × 10⁻¹ / 15.2 / 3-8	
Interval cm⁻¹	microns	Σx 100	N × 10,000	Σx 100	N × 10,000	Σx 100	N × 10,000	Σx 100	N × 10,000	Σx 100	N × 10,000	Σx 100	N × 10,000	Σx 100	N × 10,000
1950-2000	5.1282-5.0000	0.	0.	[illegible]	0	0	0	0.	0.	0	0.	0.	0.	0.	0.
2000-2050	5.0000-4.8780	0.	0.	0.	0.	0	0.	0.	0.	0	0.	0.	0.	0.	0.
2050-2100	4.8780-4.7619	0.	0.	0.30	0.017	0.16	2.007	0.75	4.555	1.66	12.1[illegible]	0.	0.	0.	0.
2100-2150	4.7619-4.6512	0.50	5.273	1.47	12.932	1.12	20.065	5.56	47.629	6.60	55.650	0.	0.	0.	0.
2150-2200	4.6512-4.5455	1.07	[illegible]	6.11	11.380	15.64	110.012	27.61	260.206	61.16	156.260	0.06	0.010	0.29	2.512
2200-2250	4.5455-4.4444	15.00	132.001	16.79	255.569	47.01	432.045	70.70	472.602	89.96	792.065	1.29	11.400	2.01	22.962
2250-2300	4.4444-4.3478	27.55	243.621	[illegible]	451.612	72.01	662.050	91.01	418.215	99.01	887.721	3.07	27.100	6.07	59.431
2300-2350	4.3478-4.2553	29.42	260.751	[illegible]	465.621	75.60	680.300	91.96	844.745	99.95	900.915	5.22	50.875	8.41	75.016
2350-2400	4.2553-4.1667	11.02	110.520	26.55	221.160	40.65	171.550	61.75	561.566	69.22	720.975	2.51	22.462	4.56	41.290
2050-2055	4.8780-4.8662	-0.	-0.	-0.	-0.	-0.	-0.	-0.	-0.	0.11	0.095	-0.	-0.	-0.	-0.
2055-2060	4.8662-4.8544	-0.	-0.	-0.	-0.	-0.	-0.	-0.	+0.	0.19	0.321	-0.	-0.	-0.	-0.
2060-2065	4.8544-4.8426	-0.	-0.	-0.	-0.	-0	-0.	0.	0.	0.66	0.556	-0.	-0.	-0.	0.
2065-2070	4.8426-4.8309	-0.	-0.	-0.	-0.	0.	0.	0.11	0.096	0.00	0.762	-0.	-0.	-0.	-0.
2070-2075	4.8309-4.8193	-0.	-0.	-0.	-0.	0.26	0.060	0.44	0.372	0.96	0.000	-0.	-0.	-0.	-0.
[illegible]	[illegible]	[illegible]	[illegible]	[illegible]	[illegible]	[illegible]	[illegible]	[illegible]	[illegible]	[illegible]	[illegible]	[illegible]	[illegible]	[illegible]	[illegible]

TABLE 3-II

Interval cm^{-1}	Interval	$\bar{E}$ * 100	N * 10,000	$\bar{E}$ * 100	N * 10,000	$\bar{E}$ * 100	N * 10,000	$\bar{E}$ * 100	N * 10,000	$\bar{E}$ * 100	N * 10,000
[illegible]	[illegible]	[illegible]	[illegible]	[illegible]	[illegible]	[illegible]	[illegible]	[illegible]	[illegible]	[illegible]	[illegible]

TABLE 3-2A

[illegible]

TABLE 3-2A (CONTINUED)

TABLE 3-2B

TABLE 3-2B (CONTINUED)

TABLE 3-2C

[illegible]	[illegible]	[illegible]	[illegible]	[illegible]	[illegible]	[illegible]	[illegible]	[illegible]	[illegible]	[illegible]	[illegible]	[illegible]	[illegible]	[illegible]	[illegible]	[illegible]	[illegible]	[illegible]	[illegible]	[illegible]	[illegible]

TABLE 3-2C (CONTINUED)

[illegible]	[illegible]	[illegible]	[illegible]	[illegible]	[illegible]	[illegible]	[illegible]	[illegible]	[illegible]	[illegible]	[illegible]	[illegible]	[illegible]	[illegible]	[illegible]	[illegible]	[illegible]	[illegible]	[illegible]	[illegible]

SECTION 4

RESULTS: EMISSION BY HOT H_2O

Results on emission measurements of 11 samples of pure H_2O vapor at 900°K, 1200°K, and 1500°K are presented in this section. Pressures were varied from approximately 48 to 760 mm Hg, with a sample cell length of 7.75 cm. Figures 4-1 to 4-5 show emissivity curves replotted from spectra obtained with resolution schedule C (Table 2-1). As in the case of the CO_2 emissivity curves a small amount of information has been lost in the replotting. In a few cases it appeared that the automatic replotter did not move in straight lines between the points on some of the steep slopes. The error tended to make the emission lines appear slightly narrower than they should. The uncertainty in the emission curves is somewhat greater on the low frequency side, below approximately 3300 cm^{-1}, than in other portions of the spectrum. The greater uncertainty in this region is due to two factors. The first is that the recorder deflection in this region is only about 30% of full scale on the original spectra. The other factor is the error in fitting the spectrum to the background because the two curves converge so gradually that it is difficult to determine where they should meet.

Results of the calculations of $\bar{\epsilon}$ and N are given in Table 4-1 in the same form as the CO_2 results in Tables 3-1 and 3-2. Information about the contents of the tables is given just previous to Table 3-1.

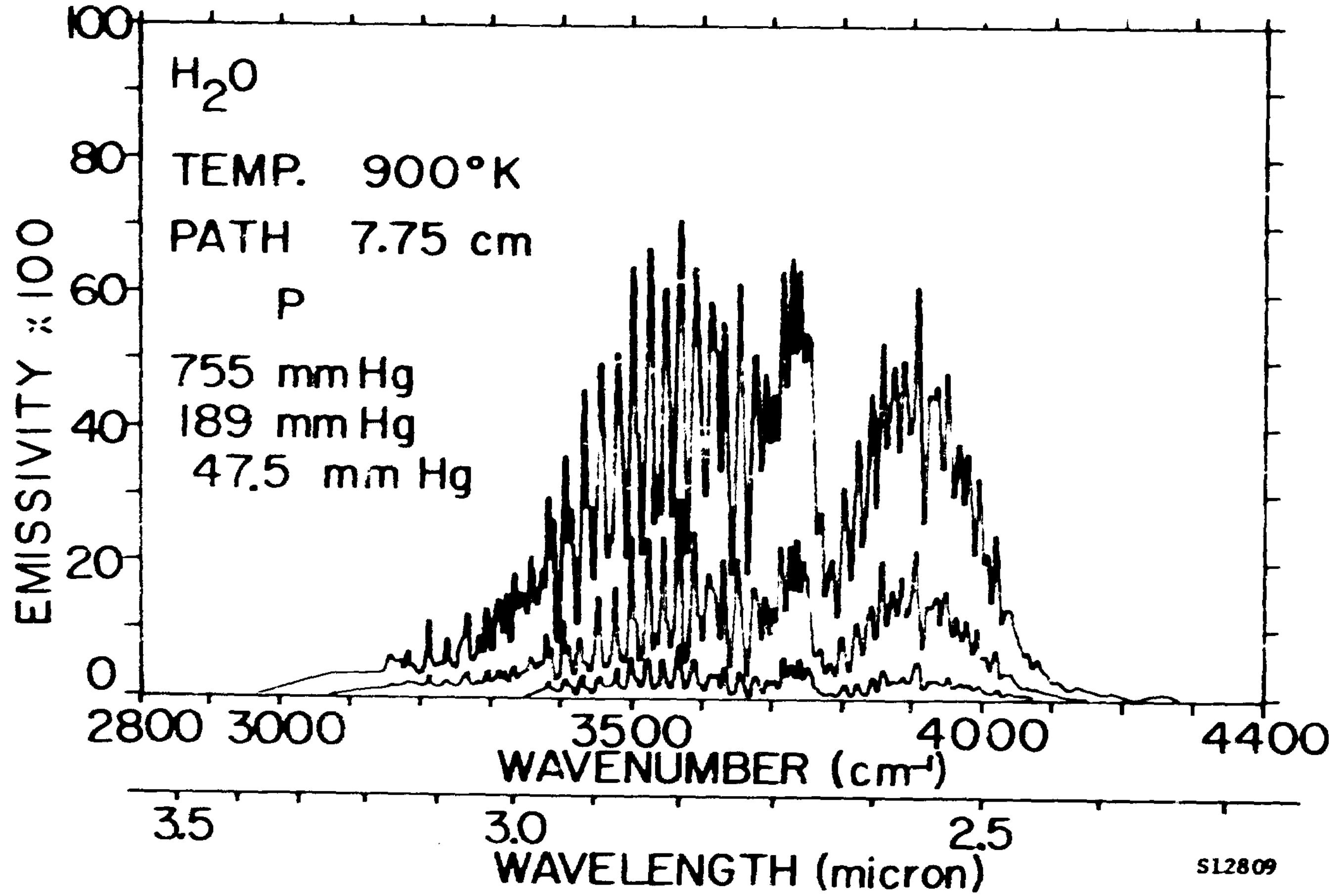

FIGURE 4-1. EMISSIVITY CURVES FOR SAMPLES W1, W3 AND W5

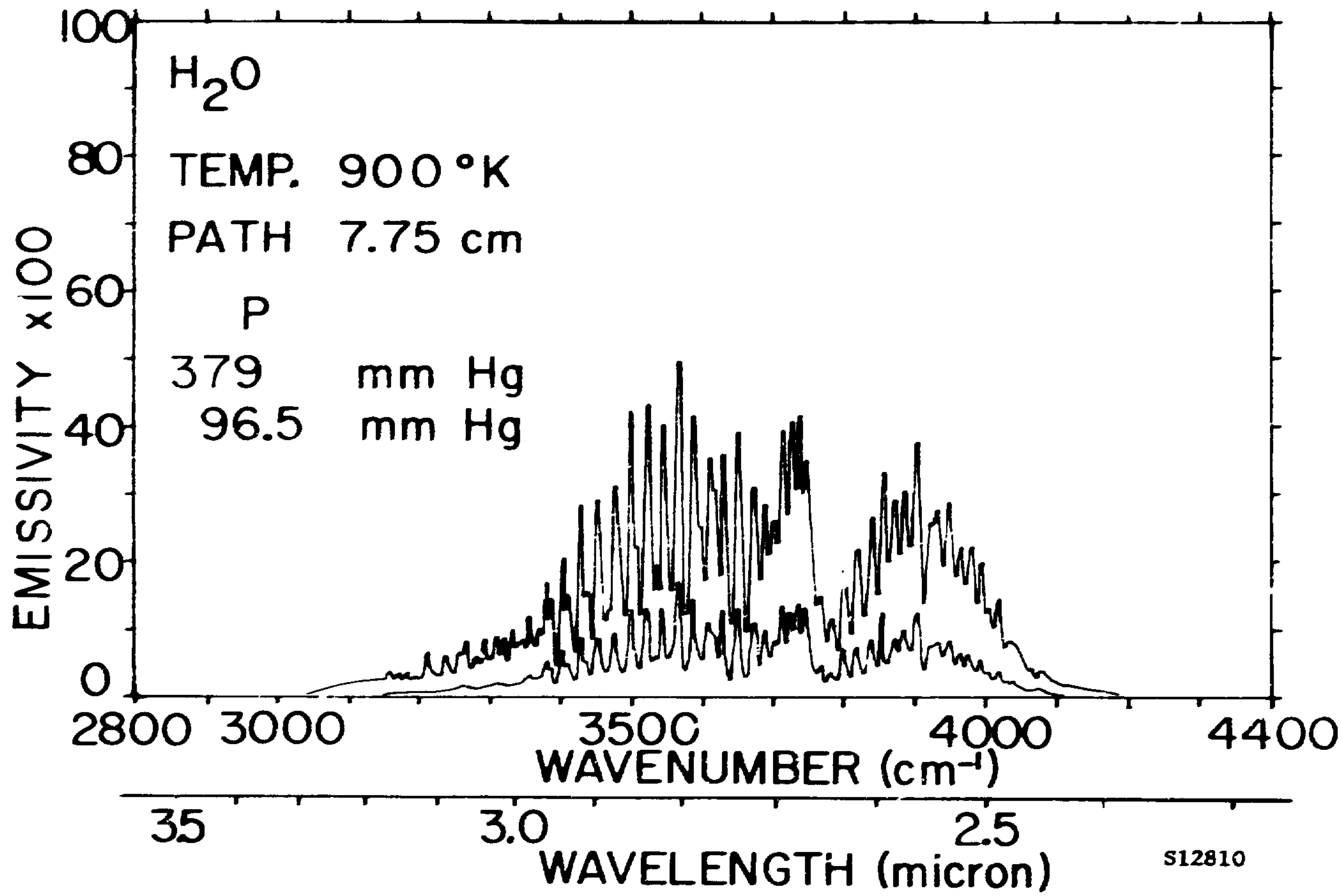

FIGURE 4-2. EMISSIVITY CURVES FOR SAMPLES W2 AND W4

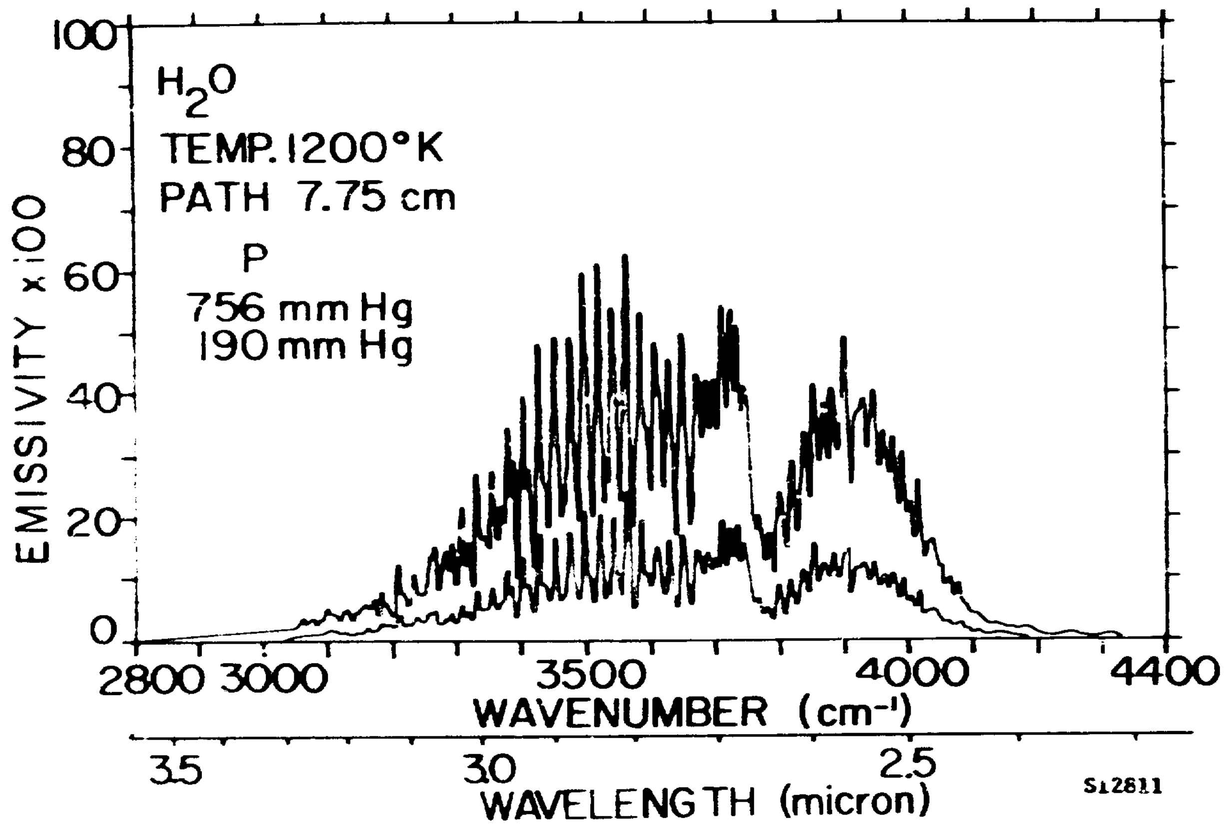

FIGURE 4-3. EMISSIVITY CURVES FOR SAMPLES W6 AND W8

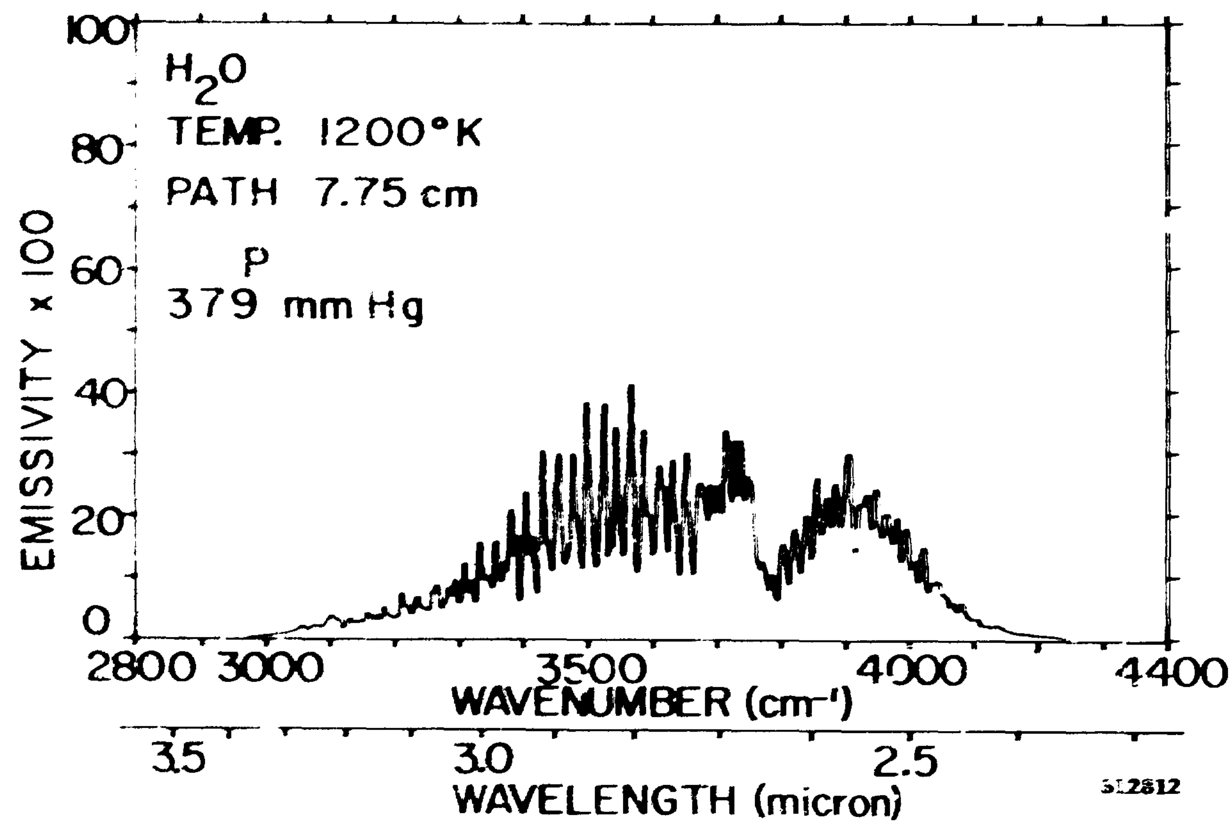

FIGURE 4-4. EMISSIVITY CURVES FOR SAMPLE #7

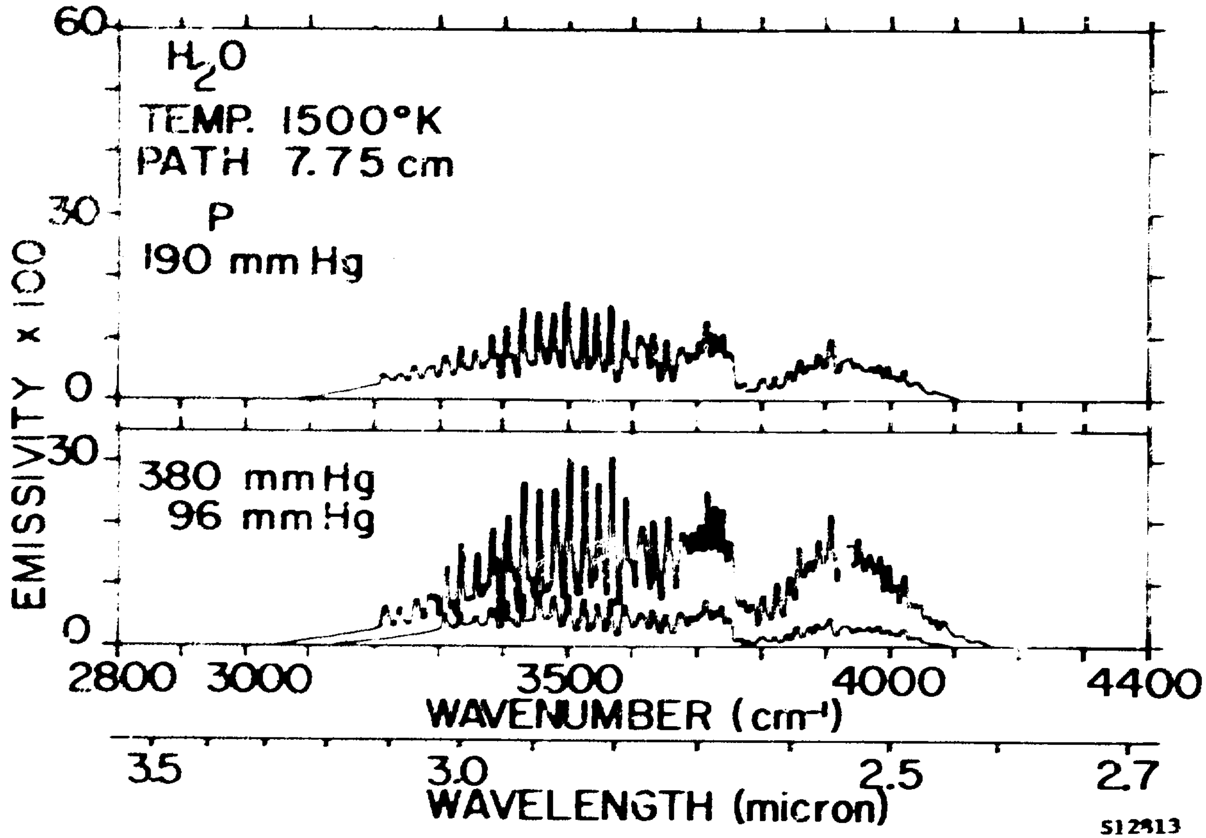

512813

FIGURE 4-5. EMISSIVITY CURVES FOR SAMPLES W9, W10 AND W11

TABLE 4-1

TABLE 4-1 (CONTINUED)

TABLE 4-1 (CONTINUED)

[illegible]

TABLE 4-1 (CONTINUED)

TABLE 4-1 (CONTINUED)

SECTION 5

TRANSMISSION OF RADIATION FROM HOT CO_2 THROUGH COLD CO_2

Introduction and Theoretical

In dealing with the detection of hot gas sources such as rocket plumes and jet exhausts, the problem of transmission of the infrared radiation through the atmosphere is as important as the problem of emission by the hot gas. This is particularly true since H_2O and CO_2, the main radiating constituents in flames also occur in the atmosphere. Since the emissivity of a gas is large at the same frequencies as the absorptance, the gases tend to radiate at frequencies where there are atmospheric absorption bands. Much work on the transmission of atmospheric gases has been done so that it is now possible to estimate the transmittance of atmospheric paths covering wide ranges of path length, pressure and atmospheric composition. From these estimates it is possible to determine the fraction of the radiant power from a source that is transmitted if the spectral radiance of the source is constant over the spectral interval being considered. However, if the spectral radiance of the source varies rapidly with wavenumber, as is frequently true for a hot gas, the amount of transmitted power cannot be determined directly from the transmission data that are available. The reason for this can be explained by the use of the simplified model illustrated in Figure 5-1.

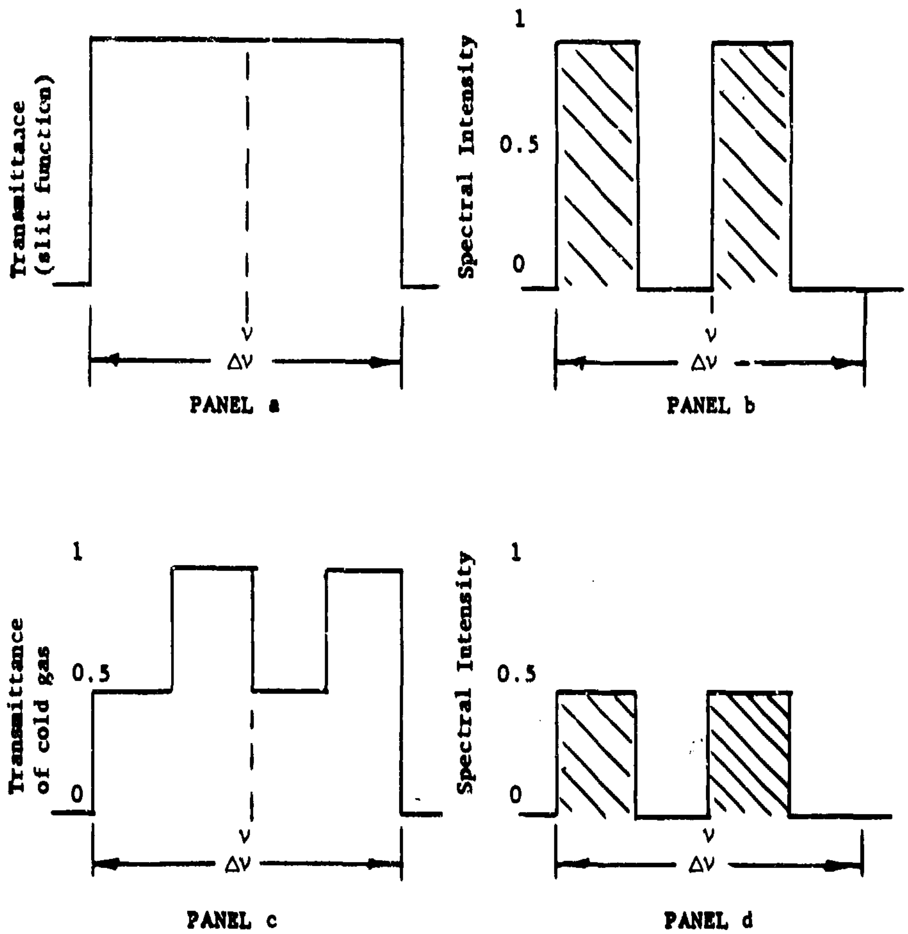

Fig. 5-1
A Simple Model Showing the Effect of Coincident Lines

The upper portion represents the slit transmission function of the monochromator, which is zero outside of the spectral interval $\Delta\nu$ wide and centered about ν. Of course, this is not a realistic slit function, but it is simple and will serve the present purpose. Panel b represents the true spectral intensity of a hot gas source having two emission lines in the interval $\Delta\nu$; each is assumed to be 0.25 $\Delta\nu$ wide and to have unit intensity in arbitrary units. In observing this source with a monochromator having the slit function indicated the emission lines would not be resolved, and with the monochromator set at ν, the signal on the

detector would be proportional to the average intensity over $\Delta\nu$. Now assume that the radiation from the hot gas passes through a sample of cold gas having a true transmittance curve like that shown in panel c of Figure 5-1. In this example the absorption lines of the cold gas are coincident with the emission lines of the hot gas. Panel d of the figure represents the spectral intensity of the transmitted radiation obtained from the product of the curves in panels b and c. The maximum spectral intensity of each line will be reduced to one-half unit, and the signal will be reduced to half its size by the cold gas. The observed transmittance of the cold gas, defined as $T_c^*(\nu)$, when used with this gaseous source of radiation is 0.5. It can be seen that if the spectral intensity of the radiation incident on the gas were constant over $\Delta\nu$, the observed transmittance $T_c(\nu)$ at ν would be 0.75, the average of the true transmittance.

Thus, it is apparent that the fraction of the radiation transmitted by a cold gas sample having unresolved "structure" is dependent on the structure of the emitting gas. In the example given here, in which the emission lines and absorption lines are coincident, $T_c^*(\nu) < T_c(\nu)$. It is apparent that if the absorption lines were displaced so that they occurred in between the emission lines, $T_c^*(\nu)$ would be greater than $T_c(\nu)$.

When observing hot CO_2, for example, through an atmospheric path containing cold CO_2, it is expected that many of the absorption lines will coincide with the emission lines, with the result that $T_c^*(\nu) < T_c(\nu)$. The problem is complicated by the fact that there are many lines which contribute significantly to the emission by hot CO_2 but are negligible in cold CO_2[9]. The relative intensities of many of the lines also change considerably as the CO_2 is heated. Thus, one expects that there would be some, but not complete, correlation between the lines of the emitting and absorbing gases.

The ideal method to investigate $T_c^*(\nu)$ and its deviation from $T_c(\nu)$ would involve a system in which a variety of cold samples could be contained in an absorption cell; and for sources of radiation one would have both a hot gas sample and a continuous source, such as a Nernst glower. It would be desirable to be able to vary the optical thickness, pressure, and temperature of the hot gas and to have it at uniform pressure and temperature. As explained in Section 1, it is not feasible to use a gas sample in the furnace as a source of radiation because of radiation from the windows; and an open flame has the disadvantage that the temperature is not uniform and there are limitations on the pressures and optical thicknesses which can be obtained.

Although it is not feasible to use a sample in the furnace as a radiation source, it is possible to make transmission measurements under some conditions which enable one to calculate the value of $T^*_C(\nu)$ for a cold sample that would be observed if the sample in the furnace were the source. The measurements are made in a manner similar to those described in Section 3 and 4, except that the optics tank is used as an absorption cell in "series" with the furnace. Absorption spectra are made in sets of three: the first with a sample in the furnace and the absorption cell evacuated; the second with the same sample in the furnace and another sample in the absorption cell. The third spectrum is then obtained with the furnace evacuated and the sample left in the absorption cell. From the three spectra, values of $T_H(\nu)$, (hot gas); $T_{HC}(\nu)$, (hot and cold gas); and $T_C(\nu)$, (cold gas), respectively, are calculated at several frequencies throughout the band. It is shown below that the value of $T^*_C(\nu)$ at these same frequencies can be calculated from

$$T^*_C(\nu) = \frac{T_C(\nu) - T_{HC}(\nu)}{1 - T_H(\nu)}. \qquad (5\text{-}1)$$

<u>Derivation of $T^*_C(\nu)$</u>

With the monochromator set at frequency (ν), $D_o(\nu)$ is the recorder deflection observed with no sample in the furnace or in the cold absorption cell, using a glower source.

$$D_o(\nu) = \int_{\Delta\nu} N(\nu)\, C(\nu)\, f(\nu)\, d\nu, \qquad (5\text{-}2)$$

where $N(\nu)$ is the spectral radiance of the glower and $C(\nu)$ is a variable quantity which depends on the aperture and transmittance of the optical system, not including the slits, and on the sensitivity of the detector and amplifying system. $f(\nu)$ is the slit function of the monochromator; i.e., the transmittance of the monochromator over the interval $\Delta\nu$ passed by the slits. If a sample of gas is put in the cold cell, with all other parts of the optical system kept the same, the recorder deflection will be given by

$$D_C(\nu) = \int_{\Delta\nu} N(\nu)\, C(\nu)\, f(\nu) \exp\left[-k_C(\nu)\, u_C\right] d\nu. \qquad (5\text{-}3)$$

$k_C(\nu)$ is the true absorption coefficient of the cold sample as would be observed with an instrument having infinite resolving power, and u_C is the optical thickness of the cold sample. With a Nernst glower and an optical system of the type used in the present investigation, it is usually safe to assume that $N(\nu)$ and $C(\nu)$ are constant over $\Delta\nu$ (from 5 to 25 cm^{-1}) and can be removed from under the integral sign.

The observed transmittance $T_C(\nu)$ is given by

$$T_C(\nu) = \frac{D_C(\nu)}{D_o(\nu)} = \frac{\int_{\Delta\nu} f(\nu) \exp\left[-k_C(\nu)\, u_C\right] d\nu}{\int_{\Delta\nu} f(\nu)\, d\nu}. \tag{5-4}$$

Similarly, the observed transmittance $T_H(\nu)$ of the hot sample alone is given by

$$T_H(\nu) = \frac{\int_{\Delta\nu} f(\nu) \exp\left[-k_H(\nu)\, u_H\right] d\nu}{\int_{\Delta\nu} f(\nu)\, d\nu}, \tag{5-5}$$

where $k_H(\nu)$ is the true absorption coefficient of the hot gas and u_H is its optical thickness.

The observed transmittance of both the hot and cold samples in "series" is

$$T_{HC}(\nu) = \frac{\int_{\Delta\nu} f(\nu) \exp\left[-k_C(\nu)\, u_C\right] \exp\left[-k_H(\nu)\, u_H\right] d\nu}{\int_{\Delta\nu} f(\nu)\, d\nu}. \tag{5-6}$$

Since we are interested in relating the quantities given by equations 5-4, 5-5, and 5-6 to $T_C^*(\nu)$, the transmittance of the cold sample that would be observed if the hot gas were used as the source of radiation, we assume another optical and detecting system which is different from the present one except that it must have the same slit function $f(\nu)$. We define D_H^{*B} as the signal or recorder deflection observed at frequency ν if a blackbody at the temperature of the hot gas were viewed through the assumed system with no absorbing gas in the beam. If we replace the sensitivity constant $C(\nu)$ in equation 5-3 by $C^*(\nu)$ then D_H^{*B} is given by

$$D_H^{*B}(\nu) = N^B(\nu)\, C^*(\nu) \int_{\Delta\nu} f(\nu)\, d\nu, \tag{5-7}$$

where $N^B(\nu)$ is the spectral radiance of the blackbody.

If the hot gas sample instead of the blackbody were viewed with the same system, the signal would be

$$D_H^*(\nu) = C^*(\nu)N^B(\nu)\int_{\Delta\nu} f(\nu) \left\{1-\exp[-k_H(\nu)u_H]\right\} d\nu, \qquad (5\text{-}8)$$

where the term in braces is the true emissivity of the hot gas. Now if the radiation from the hot gas passes through the cold gas sample, the observed signal will be

$$D_{HC}^*(\nu) = C^*(\nu)N^B(\nu)\int_{\Delta\nu} f(\nu) \left\{1-\exp[-k_H(\nu)u_H]\right\} \left\{\exp(-k_C(\nu)u_C)\right\} d\nu. \qquad (5\text{-}9)$$

By the definition of $T_C^*(\nu)$, it is given by D_{HC}^*/D_H^*. Therefore $T_C^*(\nu)$ =

$$\frac{\int_{\Delta\nu} f(\nu)\exp[-k_C(\nu)u_C] - \int_{\Delta\nu} f(\nu)\exp[-k_H(\nu)u_H]\exp[-k_C(\nu)u_C]d\nu}{\int_{\Delta\nu} f(\nu)d\nu - \int_{\Delta\nu} f(\nu)\exp[-k_H(\nu)u_H]\,d\nu}. \qquad (5\text{-}10)$$

It is noted that if each term in equation (5-10) is divided by $\int_{\Delta\nu} f(\nu)d\nu$,

$$T_C^*(\nu) = \frac{T_C(\nu) - T_{HC}(\nu)}{1 - T_H(\nu)} = \frac{T_C(\nu) - T_{HC}(\nu)}{\epsilon_H(\nu)}. \qquad (5\text{-}1')$$

Thus, it is possible by the use of equation (5-11) to determine $T_C^*(\nu)$ from the three measurements of transmittance made at the <u>same</u> value of ν. It should be noted that the measurements must be made with the same slit function; the calculated value of $T_C^*(\nu)$ then applies to the same slit function.

Since the effect of correlation between the lines appears as a difference between $T_C^*(\nu)$ and $T_C(\nu)$, the measurements are made under conditions in which this difference can be determined with reasonable accuracy. In this regard the technique described is not useful for values of $T_H(\nu)$ or $T_C(\nu)$ near zero or near unity. If $T_C(\nu)$ is near zero or unity, or if T_H is near zero, the difference between $T_C(\nu)$ and $T_C^*(\nu)$ is so small that it cannot be determined with much accuracy. If $T_H \approx 1$, a small error in its measurement will give rise to a large error in the calculated value of $T_C^*(\nu)$, since the denominator in equation (5-1') becomes small. For this reason, measurements of $T_C^*(\nu)$ have been limited to spectral regions over which $T_H(\nu)$ and $T_C(\nu)$ lie between 0.1 and 0.9. In order to investigate different spectral regions, the pressures and optical thicknesses of the samples are changed so that $T_H(\nu)$ and $T_C(\nu)$ lie within the prescribed limits in the desired interval.

In the discussion of the simple model illustrated in Figure 5-1, it was noted that $T_C^*(\nu) < T_C(\nu)$ if the emission lines are coincident with the absorption lines, and $T_C^*(\nu) > T_C(\nu)$ if the emission lines occur between the absorption lines. If the positions and strengths of the emission lines occur at random with respect to the absorption lines, then $T_C^*(\nu) = T_C(\nu)$. When $T_C^*(\nu) = T_C(\nu)$, there is said to be no correlation between the emission lines and the absorption lines. It can be seen from equations 5-1' that $T_{HC}(\nu) = T_H(\nu) \times T_C(\nu)$ under this condition.

Several measurements have been made in the spectral region near 3700 cm^{-1} with hot H_2O in the furnace and cold CO_2 in the absorption tank; and it has been found that $T_C^*(\nu) = T_C(\nu)$. This result is not surprising since it can be seen from high-resolution spectra that there is little, if any, correlation between the positions of H_2O lines and CO_2 lines. It has also been shown previously[10] that the product of the transmittances of a water vapor sample and a CO_2 sample obtained separately is equal to the product of the two samples in series, when both samples are at room temperature.

It can be seen from equation (5-6) that $T_{HC}(\nu) = T_H(\nu) \times T_C(\nu)$ if either $k_C(\nu)$ or $k_H(\nu)$ is constant over $\Delta\nu$ so that the exponential factor including it can be removed from under the integral sign. Thus, a difference between $T_C^*(\nu)$ and $T_C(\nu)$ occurs only when there is unresolved "structure" in both the emission spectrum and the absorption spectrum. It follows that $k_C(\nu)$ and $k_H(\nu)$ will be constant over one spectral slit width as $\Delta\nu$ is made very small so that it is much less than the half-width of all the lines. For the pressures, temperatures and slit widths encountered in the present study, $\Delta\nu$ is 2 or 3 orders of magnitude larger than the half-width of the spectral lines[11].

Results

In the upper portion of Figure 5-2 is shown a curve relating emissivity to wavenumber for the CO_2 sample indicated; and the solid curves in the lower portion are transmittance curves for two cold samples. The x's on the dotted curve in the lower panel represent values of $T^*_C(v)$ which were calculated for the 10 mm Hg sample if the hot sample represented in the upper panel were the source. Values of $T^*_C(v)$ were determined by inserting into equation (5-1') the measured values of $T_C(v)$, $T_H(v)$ and $T_{HC}(v)$ for the samples involved. Similarly, the +'s represent values of $T^*_C(v)$ for the 1.3 mm Hg sample with the same hot sample as the source. It is seen that $T^*_C(v)$ is considerably less than $T_C(v)$ over most of the spectral interval where it can be calculated. If one compared values of $A_C(v) = 1 - T_C(v)$ and $A^*_C(v)$ instead of $T_C(v)$ and $T^*_C(v)$, it is seen that $A^*_C(v)$ is more than twice as great as A_C over a considerable portion of the spectrum of the 1.3 mm Hg sample. The curves in Figures 5-2, 5-3, and 5-4 are based on spectra obtained with slit widths given by Resolution Schedule B in Table 2-1.

It is noted that the samples represented in Figure 5-2 are at relatively low pressures; thus one would expect the spectral lines to be narrow, giving rise to a large variation in the absorption coefficient k(v) over a spectral interval corresponding to one slit width. Since the "structure" in the band gives rise to the difference between T_C and T^*_C, one would expect this difference to be greatest for lowest pressures.

Figure 5-3 includes a similar set of curves with the hot sample composed of a dilute mixture of CO_2 in N_2, thus producing a sample of low optical thickness but high pressure. It is well known[12] from previous transmission studies that the structure of a band is decreased by increasing the pressure and decreasing the optical thickness. On this basis one would expect that the difference between T_C and T^*_C would be less for a given cold sample when the hot sample is at high pressure and low optical thickness than when the hot sample is at low pressure. Comparison of Figure 5-3 with Figure 5-2 seems to bear out this expectation in the case of the 1.3 mm Hg sample. However, the difference between T_C and T^*_C for the larger cold samples (9 mm Hg and 10 mm Hg) is not greatly different in the two figures. Since complete "smoothing" of the structure of <u>either</u> the hot or cold sample would eliminate any effect of correlation, it can be concluded from Figure 5-3 that a significant amount of structure still exists in the hot sample at a pressure of 1130 mm Hg.

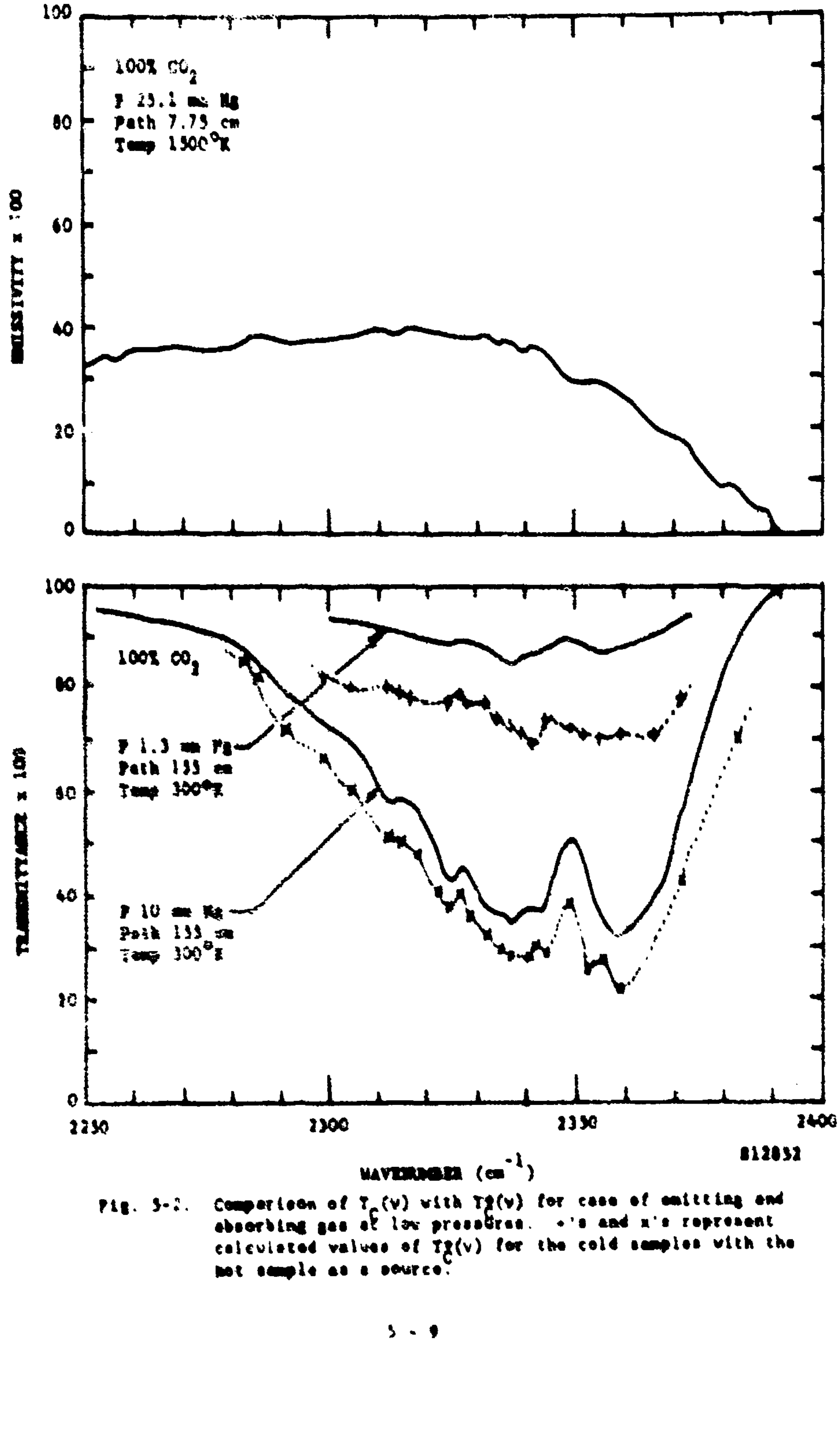

Fig. 5-2. Comparison of $T_c(v)$ with $T_c^o(v)$ for case of emitting and absorbing gas at low pressures. +'s and x's represent calculated values of $T_c^o(v)$ for the cold samples with the hot sample as a source.

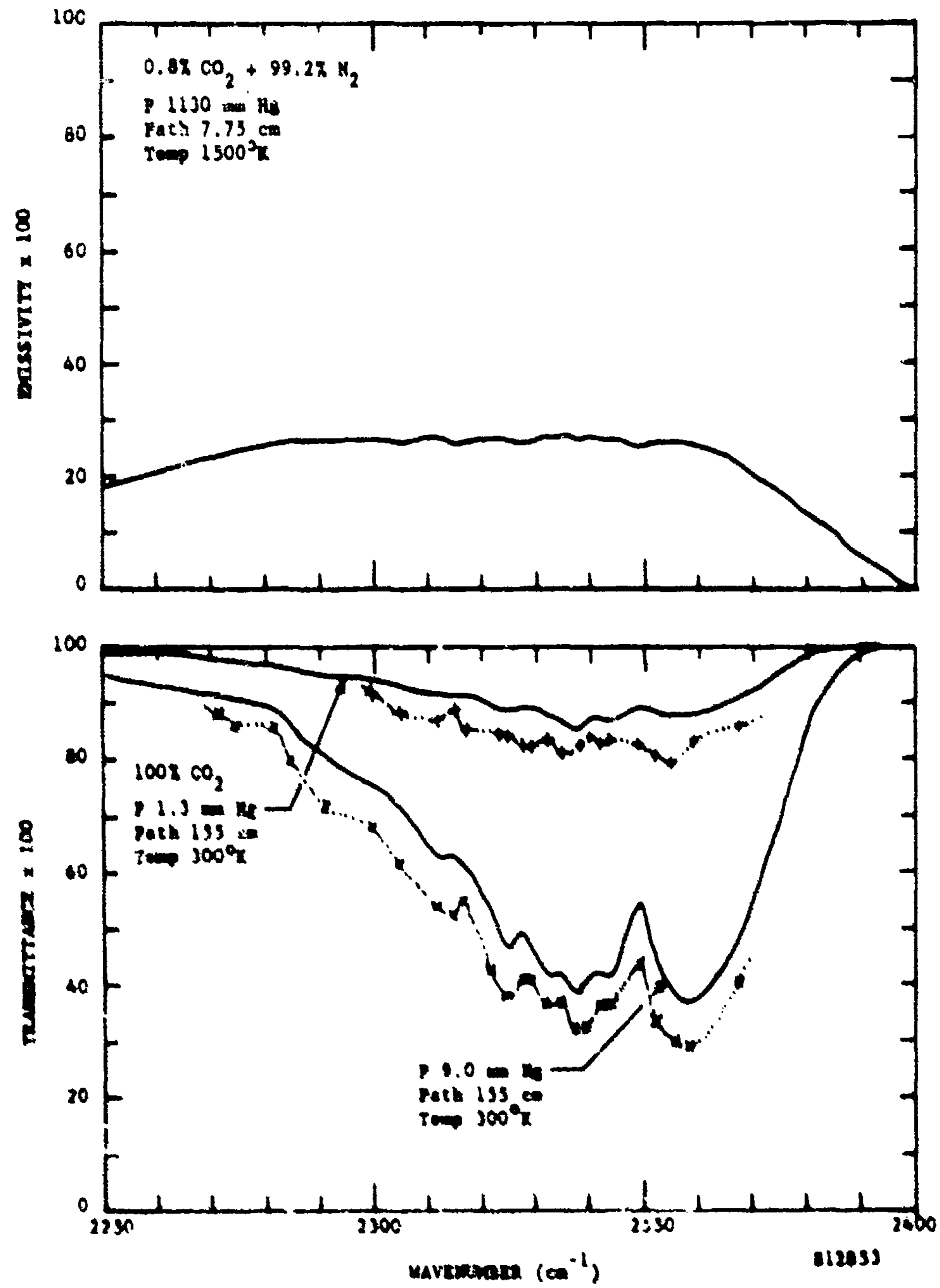

Fig. 5-3. Comparison of $T_c(\nu)$ with $T_c^o(\nu)$ for case of emitting gas at high pressure and absorbing gas at low pressure.

Figure 5-4 shows two pairs of curves obtained with larger samples to investigate the low wavenumber side of the region. The large cold samples were obtained by using the multiple-pass mirror system in the optics tank as shown in the left-hand portion of Figure 2-1. The x's adjacent to curve A (lower panel) represent calculated values of $T^*_C(\nu)$ for the same cold sample when the hot source is the one whose emissivity is shown by curve A in the upper panel. Although the calculated values appear to lie close to the steep portion of the curve, most of them lie below the curve by an amount corresponding to a difference in transmittance of approximately 0.04. This difference is believed to be significant, and one can conclude that there is some correlation between the emission lines and the absorption lines in this region.

It is noted that curve B in the lower panel contains a region of low transmittance between 2000 and 2150 cm^{-1}, but emissivity curve B in the upper panel contains no corresponding maximum. Since the gross structure of these two spectra are greatly different in this region, it is of interest to check for correlation between the emission and absorption lines. The x's adjacent to B in the lower panel represent values of $T^*_C(\nu)$ calculated by using the hot source corresponding to B in the top panel. With the exception of 2 or 3 points, the x's seem to fall very close to the curve, indicating that there is very little, if any, correlation between the positions and intensities of the lines in the two samples. This result is not surprising since the gross appearances of the spectra of the samples are greatly different, indicating that the relative contributions of the different vibration-rotation lines are different.

Figure 5-5 shows two sets of curves for the region near 3700 cm^{-1} which are based on spectra obtained with slit widths given by Resolution Schedule D in Table 2-1. As in the previous figures, the +'s and x's represent calculated values of $T^*_C(\nu)$ for the cold samples with the sample represented in the upper panel as the source. It is seen that the calculated values of $T^*_C(\nu)$ fall slightly below the curves of $T_C(\nu)$, as was found to be true for the 2350 cm^{-1} region.

<u>Future Plans</u>

The multiple-pass absorption cell having a base length of 29 meters will be used to contain samples of rather large optical thickness and very low pressure in order to investigate the "line correlation effect" under conditions where it should be greatest. The shorter cells have been used in the past because of an unusual delay in the delivery of the big mirrors for the longer cell. A flame of CO_2 produced by burning

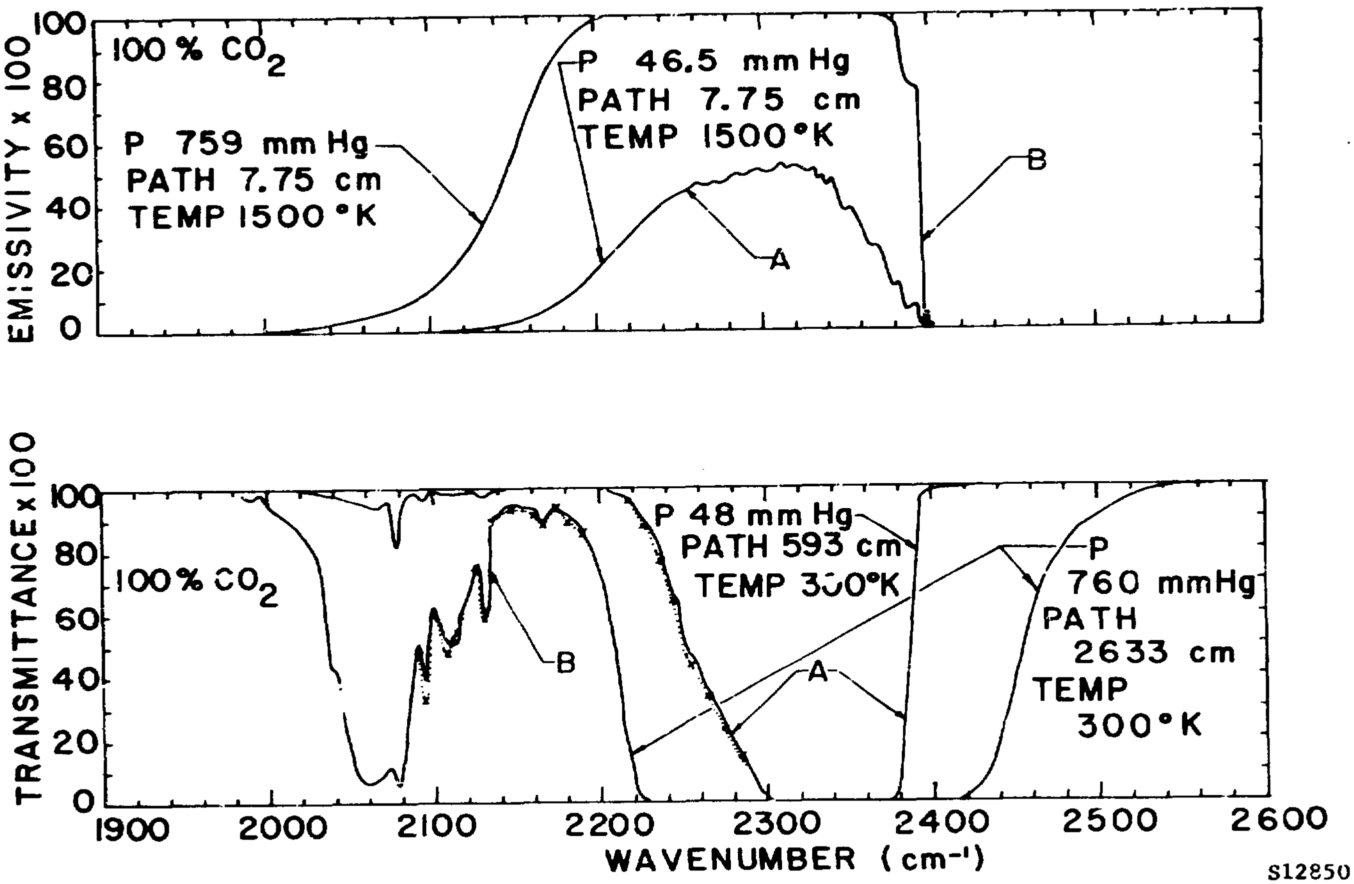

FIGURE 5-4. COMPARISON OF $T_c(\nu)$ WITH $T_c^*(\nu)$ ON THE LOW FREQUENCY SIDE OF 2350 cm^{-1} CO_2

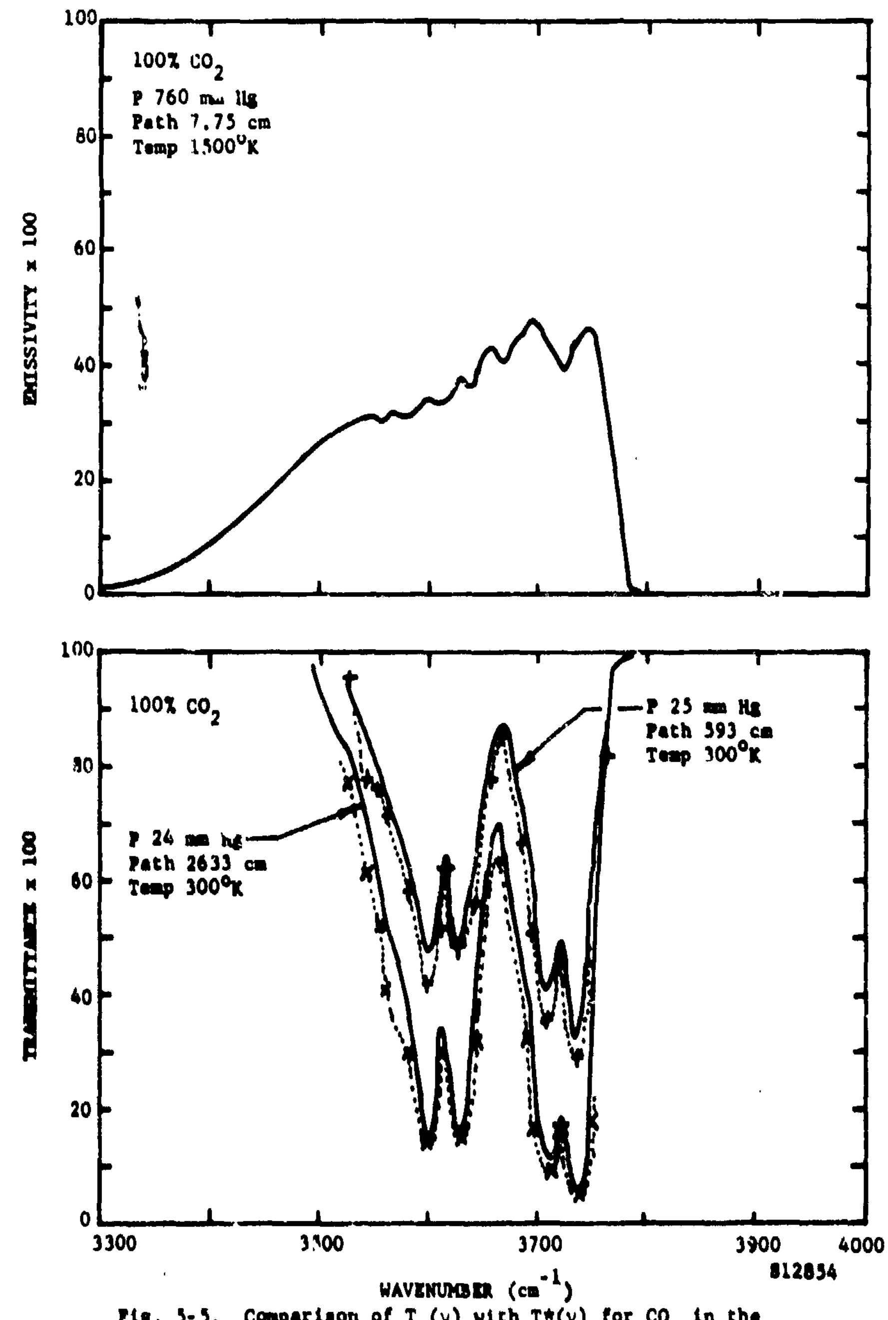

Fig. 5-5. Comparison of $T_c(v)$ with $T_c^*(v)$ for CO_2 in the $3700\ cm^{-1}$ region.

CO in O_2 will be used as an optically thin source; i.e., $T_H \cong 1$. T_C^* for cold samples can be measured directly by comparing the signal from the flame after passing through the sample, to the signal with the absorption cell evacuated. The radiation from the flame will be chopped between the flame and absorption cell.

Similar measurements will be made with H_2O samples in the long absorption cell and in the furnace. H_2O flames will be produced by burning H_2 in O_2.

SECTION 6

REFERENCES

1. Carmine C. Ferriso, "High Temperature Infrared Emission and Absorption Studies," Sci. Rept. Jan. 1961 to Aug. 1961, AFCRL, Contract AF 19(604)-5554. Several other related reports have been published by other workers at General Dynamics, including Harshbarger and Malkmus.

2. R. H. Tourin, J. Opt. Soc. Am., 51, 175 (1961).

3. D. K. Edwards, J. Opt. Soc. Am., 50, 617 (1960).

4. U. P. Oppenheim and Y. Ben-Aryeh, Reports to be published. A preliminary account of the work was given at the Ninth International Symposium on Combustion, Cornell University (1962).

5. M. Steinberg and W. O. Davies, J. Chem. Phys., 34, 1373 (1961).

6. J. U. White, J. Opt. Soc. Am., 32, 285 (1942).

7. See for example, D. E. Burch, D. A. Gryvnak, and D. Williams, Appl. Opt. 1, 739, (1962).

8. D. E. Burch, E. B. Singleton, and D. Williams, Appl. Opt., 1, 359, (1962).

9. See for example, G. N. Plass, J. Opt. Soc. Am., 49, 821 (1959).

10. D. E. Burch, J. N. Howard, and D. Williams, J. Opt. Soc. Am., 46, 452 (1956).

11. L. D. Kaplan and D. F. Eggers, J. Chem. Phys., 25, 876 (1956).

12. See for example, W. Benedict, R. Herman, G. Moore, and S. Silverman, Canad. J. Phys., 34, 830, 850 (1956).

13. The regulators are manufactured by Fisher Governor Company and sold for approximately $7.00 each.

APPENDIX A

FURNACE AND SAMPLE CELL

The furnace was designed and built as shown in Figure A-1 by the members of the Materials Department of the Aeronutronic Research Laboratories under the supervision of Dr. W. M. Fassell, Jr. and Mr. Robert Hale. It was designed to heat gas samples contained in a small cell located in the center portion of the furnace to temperatures as high as 2000°K.

Heat is provided by three resistance elements composed of Mo wire wound on McDanel AP35 alumina (Al_2O_3) tubing which has an I.D. of approximately 3.8 cm and wall thickness of 0.3 cm. The alumina tubing is more than 99% pure and is impervious. A ceramic substance which is put on in the form of a paste made from pure Al_2O_3 powder and water is used to hold the coils of the heater elements apart. Most of the heat is supplied by the main heater which is approximately 35 cm long. The other two heaters, called end-heaters, are each about 6 cm long and can be controlled independently to provide a reasonably uniform temperature. Two different sample cells have been used to date; the shorter one, which is 7.65 cm long at room temperature, can be heated to 2000°K with a maximum temperature variation of $\pm$ 5°K along the length of the cell. It is not possible to maintain this good a temperature uniformity with the longer cell (30.6 cm) above approximately 1500°K.

The portion of the furnace surrounding the sample cell is filled with argon, which is infrared inactive, in order that there be no absorption or emission in the sections where there are large temperature gradients. The pressure in the "argon section" is maintained approximately equal to that in the sample cell in order to minimize leakage between the two sections and to avoid rupturing of the very thin sapphire windows on the sample cell. During operation the argon is flushed continuously, entering one end and leaving the other.

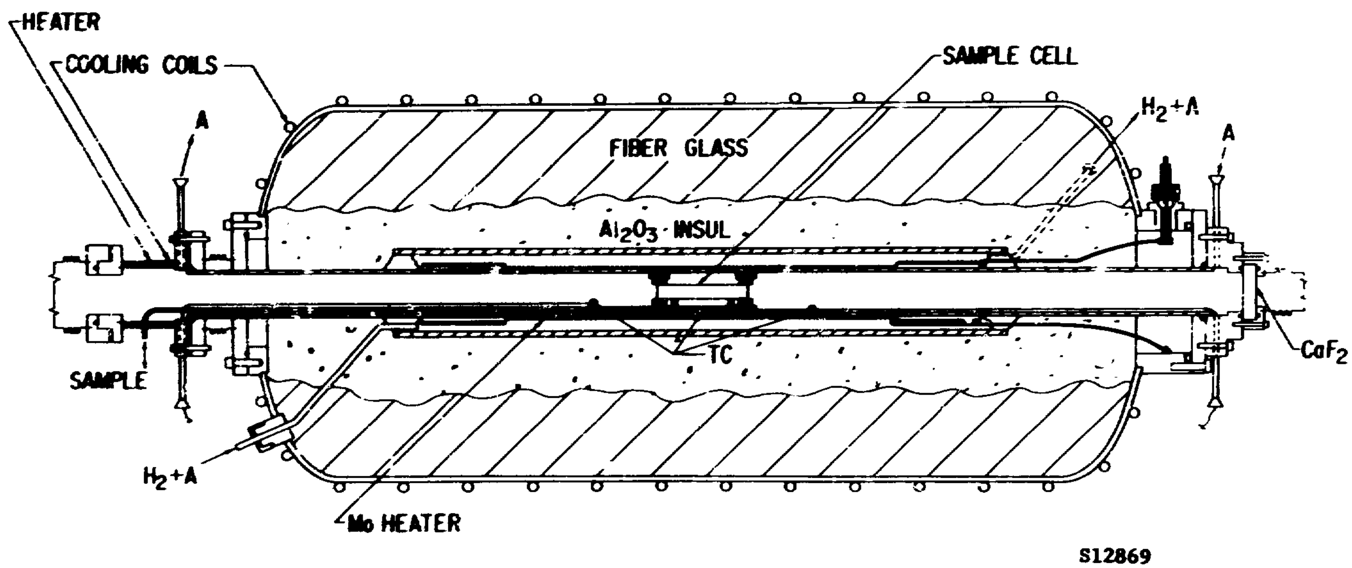

FIGURE A-1. DIAGRAM OF FURNACE AND SAMPLE CELL

The furnace can be joined to the source tank and optics tank by flexible bellows as shown in Figure 2-1. CaF_2 windows are used on the ends of the furnace where the temperature does not exceed 600 to 700°K. "O"-rings of silicone rubber are used as seals between the different sections of the furnace and as gaskets for the windows.

The heating coils are protected on the outside by a larger Al_2O_3 tubing. Around this tubing are placed Al_2O_3 pellets for insulation in the region where temperatures are too high for fiberglass, which is used in the outer part of the furnace. The cylinder containing the Al_2O_3 tubing and insulation is made of steel approximately 0.6 cm thick and is approximately 80 cm long. As indicated in the left-hand portion of Figure A-1, the center piece of alumina tubing is connected to the steel inder by use of two flanges joined by flexible bellows in order to provide room for expansion.

The section which is outside of the core of the furnace and contains the insulation is sealed from the atmosphere and from the center section of the furnace. In operation this portion is flushed with a mixture of 10% H_2 and 90% argon at a rate of approximately 1 liter per minute. This gas mixture, which is directed past the windings as indicated in Figure A-1, is used to provide a reducing atmosphere around the Mo windings to prevent oxidation. The pressure of the H_2 + argon mixture can be controlled, during flow, from approximately 50 to 1500 mm Hg. At temperatures higher than about 1500°K the pressure is maintained approximately equal to that in the argon section to minimize strain on the alumina tubing arising from any difference in gas pressure across it. It has been found that at temperatures below 1500°K the alumina tubing can safely withstand a pressure difference of 1 atmosphere. As the H_2 + argon mixture is flushed, it is pumped through a vacuum pump whose exhaust is directed into the flame of a Meeker burner where the H_2 is burned. The flame is located under a hood so that the fumes are exhausted to the outside. It was found that this technique was more reliable than attempting to burn the H_2 + argon mixture alone, since the flow was so small that the flame frequently extinguished itself.

Copper coils have been soldered to the outside of the furnace to provide water cooling. Other coils, part of which are not shown in Figure A-1, have been provided to cool the ends of the furnace so that the "O"-ring seals and CaF_2 windows will not be damaged. The separate set of heating coils which are shown adjacent to the cooling coils on the left end of the furnace are provided to heat the sample entrance and exit lines to a sufficiently high temperature to prevent condensation of H_2O when it is being studied. In some cases the extra heat is necessary when there is not enough provided by the heating elements inside the furnace. It is seen from Figure A-1 that the sample entrance and exit lines pass through this portion of the furnace.

Temperatures inside the furnace are measured by thermocouples having one leg of Pt-6% Rh and the other leg of Pt-30% Rh. The thermocouples are placed along the furnace at various locations to provide information about the temperature uniformity. Three thermocouples are indicated in Figure A-1, although additional ones have recently been used to provide more information about the temperature profile in the furnace, particularly near the windows of the sample cell and near the "O"-rings close to the ends of the furnace. In order to minimize temperature gradients within the alumina tubing, the temperatures in the regions near the "O"-ring seals are not kept much lower than is necessary for the protection of the seals. Thermocouple wires and connections to the electrical heating element are made through Conax fittings.

The voltage from the center thermocouple is recorded on a Leeds and Northrup strip chart recorder and also serves as the input to a Leeds and Northrup control unit. Voltages from the other thermocouples are measured with a vacuum tube voltmeter having very high input impedance. The controller can be preset to a given voltage corresponding to the desired temperature, and will automatically maintain this temperature after making certain adjustments which depend on the time lag between the heating coils and the thermocouple, and on the heat capacity of the system. After the furnace has been heated to the desired temperature and the controller adjustments have been made, the current through the end heaters is controlled manually to provide uniform temperature over the region containing the sample cell.

Both of the sample cells are made of an alloy of Pt-20% Rh which will withstand temperatures as high as 2000°K. The body of each cell is a piece of tubing having a wall thickness of 0.38 mm with flanges, which are 0.25 mm thick and 2.5 cm in diameter, fused to the ends. The diameter of the short cell is 1.3 cm, and the long one is 1.7 cm. Two tubes having approximately 4 mm I.D. are fused to the body of the cell, as shown in Figure A-1, and extend to one end of the furnace where they connect to the gas handling system. One tube serves as the inlet and the other as the outlet for the sample gas.

No information about the thermal coefficient of expansion of the Pt-20% Rh alloy for temperatures above about 1200°K could be found, so in order to calculate the cell length at high temperatures it was assumed that the thermal coefficient at high temperatures was the same as that at lower temperatures. Since the difference in length at the different operating temperatures is small and since it could not be calculated accurately, a single value of cell length is used for all the high temperatures. The shorter cell was the only one used in obtaining data appearing in the present report; its estimated length of 7.75 cm is probably in error by less than ± 0.05 cm.

Sapphire windows, which are 25 mm in diameter, are clamped against the flanges by the use of washers and bolts made of the same alloy as the body of the cell. Gaskets of the same material, and 0.025 mm thick, are used between the windows and the thin flanges which are sufficiently flexible to bend to the proper shape and make good contact as the windows are tightened. The seal which is formed would not be good for vacuum applications, but the leakage is small since the pressure is the same on both sides of the window. Both the sample gas and the argon are flushed continuously to avoid accumulation of either of these gases in the wrong section; i.e., the sample in the argon section or the argon in the sample cell. Flow rates of approximately 5 and 700 cm^3 per minute were used for the sample and argon, respectively.

Since the absorption by sapphire becomes important below approximately 2200 cm^{-1} ($\lambda > 4.5\mu$), the windows are as thin as seems practical. It is essential that the absorption not be large at these frequencies so that the low frequency side of the CO_2 absorption region can be studied. The absorption by sapphire increases with temperature, so the windows on the short cell, which is heated to 2000°K, are only 0.5 mm thick. Windows 1 mm thick are used on the longer cell since it will not be used at such high temperatures. As well as the need for extra strength, a further reason for using the 1 mm windows instead of the 0.5 mm ones where it is possible, is that the thinner ones produce a slight fringe pattern which can be troublesome. It is necessary to slightly defocus the optics to eliminate the fringes which appear on the spectra in the region near 2350 cm^{-1}.

APPENDIX B

GAS HANDLING SYSTEM

The most important purposes and requirements of the gas handling system are:

1. To produce samples containing H_2O, CO_2, N_2 and other non-corrosive gases in any desired mixing ratio at pressures from approximately 3 to 1500 mm Hg.

2. To continuously flow the sample gas through the sample cell at a known and adjustable rate while the pressure is automatically controlled.

3. To flow argon through the section of the furnace surrounding the sample cell at a known and adjustable rate and at the same pressure as the sample.

4. To provide a means of measuring the sample pressure with good accuracy.

5. To "bleed off" gas from either the argon or sample line after it has passed through the furnace and to direct it into the monitor cell where its infrared spectrum can be obtained.

Two key parts of the gas handling system are the inexpensive pressure regulators which were made for use on commercial gas lines[13]. The regulators are shown symbolically by parts 8 and 13 in the diagram of the gas handling system shown in Figure B-1. The pressure on the downstream side of the regulator is automatically maintained at some value p(con) provided it is less than the pressure on the upstream side. Gas flow through a small orifice is controlled by a plunger which is actuated by a mechanical connection to a diaphragm which is approximately 15 cm in diameter. One side of the diaphragm is open to the downstream side of the regulator and is, therefore, at the same pressure. The pressure on the other side of the diaphragm is defined as the reference pressure, p(ref), and is equal to the atmospheric pressure in the normal operation of the regulator on commercial gas lines. The diaphragm is spring-loaded so that a variable force can be applied to it. By varying the force against the diaphragm, the difference

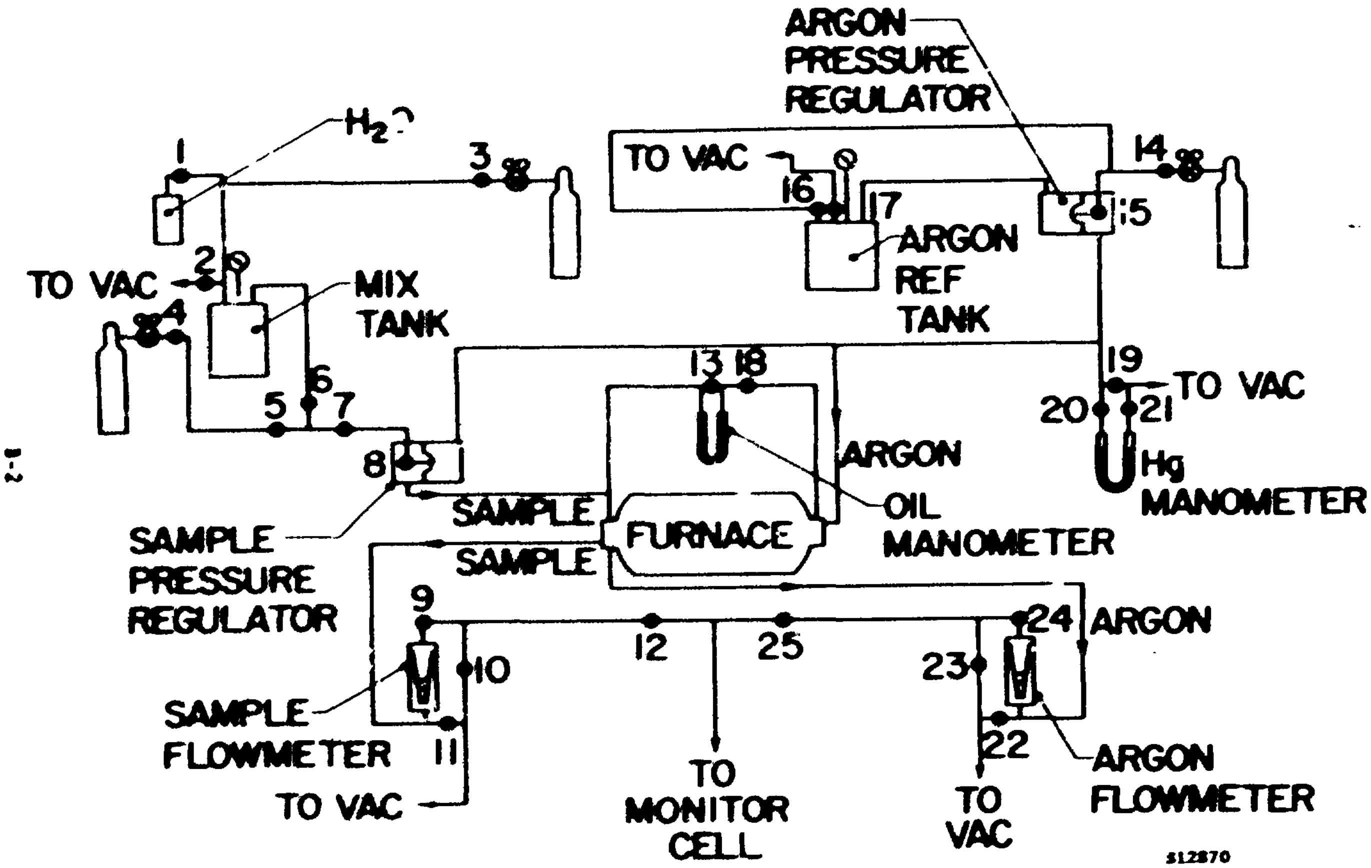

FIGURE B-1. DIAGRAM OF GAS HANDLING SYSTEM

between p(ref) and p(con) is changed. In the normal operation on commercial gas lines p(con) is from 5 to 15 mm Hg greater than p(ref). Without changing the regulator, it is not possible to adjust the force on the diaphragm so that p(ref) and p(con) are equal.

In order to use the regulators in the present investigation, two basic modifications were made. The first modification made it possible to adjust the difference between p(con) and p(ref) so that the two were equal. This was done by attaching a steel plate as a weight to the diaphragm of the regulator. The regulator was then inverted from its normal operating position, and by adjusting the force on the spring against the diaphragm, the difference between p(con) and p(ref) could be adjusted. The difference can now be regulated from approximately -5 mm to +5 mm Hg.

The second modification involved sealing the reference side of the regulator and connecting it to a tank, called the reference tank, which has a volume of approximately 6 liters. The purpose of the reference tank is to increase the volume of gas on the reference side of the diaphragm so that small leaks and motions of the diaphragm will have little effect on the reference pressure. The reference tank can be evacuated or pressurized, and the approximate pressure can be read from a dial type vacuum-pressure gauge. From the discussion of the operation of the system which follows, it can be seen that it is not necessary to know the pressure in the reference tank very accurately.

The difference between p(con) and p(ref) can be adjusted while the system is under vacuum or under pressure by changing the force of the spring against the diaphragm by means of an adjustment through a rotating seal. During operation only very small adjustments have been found to be necessary. Because of the large area of the diaphragm, the regulator will respond easily to pressure changes which are much less than 0.1 mm Hg.

The operating principles of the gas handling system can best be explained by describing the filling operation. The reference tank, the argon section, and the sample cell are all evacuated, and the valves to the vacuum pumps are all closed. Argon or air is then allowed to flow slowly into the reference tank. As the pressure in the reference tank increases the argon regulator (15) opens and argon flows into the argon section, maintaining a pressure nearly equal to the reference pressure. The argon line is connected to the reference side of the sample pressure regulator (8) so that as the argon pressure increases the regulator opens and sample gas is allowed to flow into the sample section. If the pressures are increased slowly, and if the spring force on the diaphragms of the regulators are properly adjusted, the pressures in the sample section and the argon section will be approximately equal to that in the reference

tank at all times. When the desired pressure is reached, valve (16) to the reference tank is closed. Valves (10) and (23) are then opened and needle valves (9) and (24) are adjusted to give the proper flow in the sample and argon sections, respectively. Values of flow rates are read from the flowmeters shown. Valves (10) and (23) are block valves used to stop the gas flow without closing the needle valves, thus avoiding possible damage to them. Valves (11) and (22) are open only when the system is being evacuated in order to pump the gas through the flowmeters. Valves (12) and (25) are also normally closed, and their purpose will be described below.

The small oil manometer which is connected between the sample line and the argon line serves two purposes. Valve (13) is normally closed and valve (18) open so that the manometer reads the difference in pressure between the sample and argon sections. The pressures can easily be equalized by adjusting the spring force on the diaphragm of the sample pressure regulator (8). The second purpose of the manometer is that of a safety valve; in case of a mistake in opening or closing of the other valves a large pressure difference cannot be built up between the argon and sample sections. As the pressure difference starts to increase, the oil will flow out of the manometer and into a trap which is not shown in the line. The argon and sample sections are then connected together and the pressures will quickly equalize. When the system is being evacuated, valve (13) is opened in order to maintain nearly equal pressure in the argon and sample sections without the possibility of forcing the oil from the manometer into the traps.

The pressure in the argon section is measured by one of three pressure gauges. The Hg manometer which is shown in Figure B-1 is used for pressures between 20 and 800 mm Hg. Two other gauges, which are not shown in the figure, are used for other pressure ranges. A Dubrovin is employed for pressures less than 20 mm Hg and a Bourdon type gauge for pressures greater than about 800 mm Hg. Since the sample and argon are maintained at the same pressure, the pressure indicated by the gauges is that of the sample. Possible error in the measurement of the sample pressure resulting from pressure drops in the gas lines is only important for pressures less than about 6 or 8 mm Hg for the flow rates used in the present investigation.

Samples can be introduced to the system from commercial cylinders through valves (4) and (5), or from the mix tank through valve (6). Many of the CO_2 + N_2 mixtures were purchased premixed so that they could be used directly from the cylinders. Other gas mixtures, including all those that contain N_2O, were made in the mix tank, which has a volume of about 50 liters and is lined with glass on the inside to reduce adsorption of

gas on the walls. In order to ensure proper mixing, a mixer has been incorporated in the tank. It is driven through a rotating seal by an electric motor on top of the tank.

The mix tank, small oil manometer, sample regulator, sample flowmeter, and all the other components which might contain H_2O vapor when it is being studied, are enclosed in an oven which can be heated to approximately 140°C. By maintaining this temperature it is possible to study samples containing H_2O vapor at partial pressures as high as approximately 1500 mm Hg without condensation. The lines connecting the sample cell in the furnace to the components enclosed in the oven are insulated and heated by an electric heating wire. The valves and the regulator in the oven can be controlled from outside and the oil manometer and sample flowmeter can be viewed through windows. When studying samples not containing H_2O, the components in the oven are not heated.

When a gas mixture is being produced in the mix tank, each gas is introduced separately, and the pressure is measured after each is introduced. A dial gauge connected to the mix tank gives only approximate pressures, particularly when the tank is hot. More exact values of pressure are measured by a system which is not included in Figure B-1. If the mixture does not contain H_2O vapor, the pressures are measured by one of the three gauges used on the argon line. When H_2O vapor is included in the mixture, the mix tank is connected to one side of a small glass U-tube containing vacuum pump oil which is enclosed in the oven to prevent condensation of the H_2O. The other side of the U-tube is connected to one of the three pressure gauges used on the argon line. The pressure in the line to the gauge's can be adjusted so that there is no pressure difference between the two sides of the U-tube. The gauges then indicate the pressure in the mix tank. By this technique it is possible to measure pressures in the mix tank with about the same accuracy as in the argon line without heating the pressure gauges.

Other sections of this report contain discussions of the use of the monitor cell to determine the purity of the gas coming from either the argon section or the sample section. To investigate the gas in the argon section, for example, the monitor cell is first evacuated and the gas is introduced through valve (25) with valves (23) and (22) closed. In this manner it is possible to fill the cell with a minimum of disturbance or change in the flow of the gas in the system. By adjusting the opening of valve (24) the flow of argon can be maintained very nearly constant until the pressure in the monitor cell approaches that in the argon section. When the flow stops, it is assumed that the pressure in the monitor cell is equal to that in the argon section. Valve (25) is then closed and the other valves are re-adjusted to give the desired flow rate. In order to investigate the gas in the sample section, a similar procedure is followed by use of valves 9, 10, 11, and 12.

DISTRIBUTION

	Number of Copies
Advanced Research Projects Agency Washington 25, D. C.	2
Institute for Defense Analyses 1666 Connecticut Avenue, N. W. Washington 9, D. C. Attn: RESD Library	1
University of Chicago Laboratories for Applied Sciences Museum of Science and Industry Chicago 37, Illinois Attn: L. Biberman	1
University of Michigan Institute for Science & Technology P. O. Box 618 Ann Arbor, Michigan	2
Stanford Research Institute Menlo Park, California	1
Massachusetts Institute of Technology Lincoln Laboratories Lexington, Massachusetts Attn: WS461 Office	1

	Number of Copies
General Dynamics/Astronautics P.O. Box 1128 San Diego 12, California Attn: F. Michael Dr. A. E. Green	2
Bendix Systems Division 3300 Plymouth Road Ann Arbor, Michigan Attn: D. Lowe	1
Hughes Aircraft Co. 11940 W. Jefferson Blvd. Culver City, California Attn: S. Dorfman	1
Space Technology Laboratories Space Park Redondo Beach, California Attn: A. Fulton	1
ASTIA Arlington Hall Station Arlington 1, Virginia	10
Arthur D. Little, Inc. 500 Sansome Street San Francisco, California Attn: H. Blau	1
Boeing Aircraft Co. Aerospace Division P.O. Box 3707 Seattle 24, Washington Attn: R. McDonald	1
Lockheed Missile & Space Company Sunnyvale, California Attn: H. Batten	1
Baird-Atomic, Inc. 33 University Road Cambridge 38, Massachusetts	1
Aerojet-General Corporation Azusa, California Attn: Dr. J. A. Jamieson	1

Number of Copies

National Bureau of Standards 1
Boulder Laboratories
Boulder, Colorado
Attn: Dr. D. M. Gates

Commanding Officer 1
Naval Ordnance Test Station
Weapons Development Department
China Lake, California
Attn: D. K. Moore

National Aeronautics and Space Administration 1
Goddard Space Flight Center
Greenbelt, Maryland (Unclassified Reports Only)

U.S. Weather Bureau 1
National Weather Satellite Center
Washington 25, D. C.
Attn: Dr. S. F. Singer (Unclassified Reports Only)

Chief Superintendent 1
Canadian Armament Research & Development
Establishment
P.O. Box 1427
Quebec, Canada
Attn: Dr. C. Cumming

Aerospace Corporation 3
2400 El Segundo Boulevard
El Segundo, California
Attn: Dr. C. Sherwin
H. Wesseley
I. Spiro

The Rand Corporation 2
1700 Main Street
Santa Monica, California
Attn: Dr. S. Passman
Dr. D. Deirmendjian

Denver Research Institute 1
University of Denver
Denver, Colorado
Attn: D. Murcray